Characterizing the genetic and morphological responses to a changing environment in *Strongylocentrotus purpuratus*

by

Emily Margaret Wilkins

A thesis submitted to the Graduate Faculty of
Auburn University
in partial fulfillment of the requirements of the
Degree of Master of Science

Auburn, Alabama
May 4, 2024

Keywords: Marine heatwaves, larval morphology, immune response, DNA methylation, *Strongylocentrotus purpuratus*

Approved by

Katherine Buckley, Chair, Assistant Professor of Biological Sciences
Brian Counterman, Associate Professor of Biological Sciences
Marie Strader, Assistant Professor of Biological Sciences

Abstract

Anthropogenic climate change has increased the frequency and intensity of marine heatwaves which may broadly impact the health of marine invertebrates. Rising ocean temperatures lead to increases in disease prevalence in marine organisms. Thus, it is critical to understand how marine heatwaves impact the host immune response. Epigenetic modifications such as DNA methylation are a way in which organisms are able to respond to these fluctuations in environmental conditions. However, to understand how organisms utilize these epigenetic modifications in response to environmental stress, we first must identify if and how these patterns change across early life stages under ambient conditions.

In Chapter 1, I assessed the role of environmental temperature on the development of larval immune cells in the purple sea urchin *(Strongylocentrotus purpuratus)*. I found that larvae raised in elevated temperatures have more pigment cells and are slightly larger compared to those raised at ambient temperature. Further, significant variation is observed in larval phenotypes among unique genetic crosses, highlighting the importance of genotype in structuring how the immune system develops in the context of the environment. Overall, these results suggest that developmental temperature plays a role in shaping the development of the larval immune system and may adversely affect survival long-term.

In Chapter 2, I identified how DNA methylation patterns vary throughout various stages of *Strongylocentrotus purpuratus* development, and whether genotype influences these methylation patterns, or if they are stage specific. I found both significant differences between DNA methylation patterns between developmental stage and genotype, indicating an interactive relationship between the two. Additionally, I identified differentially methylated CpG sites (DMCpG), with most sites occurring in the intergenic regions of the genome. Additionally, gene-

specific DMCpGs were identified, with genes associated with molecular functions, such as genes associated with protein binding and the structural constituent of chromatin, significantly enriched. These results provide novel insights into the variation in DNA methylation profiles between genotypes and developmental stage of an important marine invertebrate.

Overall, my thesis provides fundamental, however critical, insights into developmental variability and responses of *Strongylocentrotus purpuratus* larvae and illuminates the variation in DNA methylation patterns across critical developmental stages. Together, these results show the interplay of genotype and developmental condition on the success of *Strongylocentrotus purpuratus*.

Acknowledgements

When deciding to attend graduate school to obtain my master's degree, I had no idea the incredible journey I was about to embark on. These past three years have been some of the most taxing, stressful, but immensely rewarding years of my life (so far), and I would not trade this experience for anything. I have had the absolute privilege of not having to navigate this journey alone, and I would like to use this space to thank the people who have helped me, supported me, and loved me along the way. I am in no way good at being concise, and as not to break tradition, I will not be in my thanks.

I would first like to thank my incredible lab mates, past and present, for their amazing friendship during my time at Auburn; Sarah Leinbach of the Strader Lab, Madilyn Miller, Amelia Williams, Jake Tatum, Yu Sun, Nick Kraieski, Che Ka, Tyler Smith, and Megan Maloney of the Buckley Lab. You all have made this experience truly unforgettable, and I will look back with such fond memories of our time and adventures together. Thank you for the endless laughter and for being my biggest cheerleaders. I can't wait to see where our journeys take us.

I would specifically like to thank Megan for being by my side throughout my entire journey at Auburn. Thank you for teaching me how to design and build a tank system from scratch (I still have the scar from our first attempt at my tanks), for proofreading all of my emails and documents, and for listening to me tell the same story six times, but still acting just as interested as the first time I told it. Thank you for letting me be your "field assistant" so I could get my fix of field work, and for always lending an ear when I needed to vent or have a gab. Most importantly, thank you for your unwavering friendship and support these past few years, I am so lucky to have you in my life.

To my friends outside of Auburn, Vanessa Coggin, Megan Mannino, Meghan Bennett, Christian Franklyn, and Sarah Kramer; thank you for supporting me throughout this journey and for your frequent check-ins (especially when I go radio silent). Thank you for reminding me that there is a life outside of my academia bubble.

To Dr. Kate Buckley for her incredible mentorship, guidance, and endless support. She challenges me to be the best scientist and researcher and pushes me to be the best version of myself every day. Thank you for always being willing to drop everything to help me with problems large and small, or to listen when I need to talk something out. I am honored to have had the opportunity to be mentored by you and am so appreciative for all that you have done for me.

To Dr. Marie Strader for inspiring me to take the leap from corals to echinoderms. Thank you for believing in me and for taking a chance on me as a new graduate student, and for continuing to support me after transitioning to Texas A&M. Your continual mentorship and guidance means so much, and I am so grateful for all that you have done for me. It has been a privilege to learn from you.

Thank you to Dr. Brian Counterman and Dr. Moisés Bernal for your guidance, mentorship, frequent check-ins, and for always having your door open. Thank you to Dr. Todd Steury and Dr. Dan Warner for their statistical analysis council for Chapter 1, and to Dr. Gretchen Hofmann of UCSB for providing the sea urchins used for Chapter 1. Of course, I would be amiss if I did not thank the sea urchins for being objectively the best model organism (particularly the baby™) and for wearing the 3D printed hats I put in the tanks.

There are approximately 171,476 words that encompass the English language, however, there is no correct combination to properly express the immense love and gratitude that I have

for my family. They have been my rock throughout this whole experience, and I most certainly would not be where I am today without their unconditional love and support. I would like to thank my father, Steve, for constantly making me laugh, especially on my hardest of days. He reminds me daily to enjoy the journey and not be so focused on the destination, and his words of wisdom and encouragement have propelled me throughout my masters. My sister, Christina, for pushing me to be the best version of myself everyday – and for being the most incredible role model to look up to these past 27 years. She is fiercely driven and the hardest worker I know, and I definitely hit the jackpot in the older sister department. To my mother, Linda, who is the most selfless woman on the planet. Thank you for being my rock, and for always answering my calls/FaceTimes/texts no matter what time it is (especially the 11PM freakout after seeing my first cockroach). Every day I strive to be half the woman you are, and I am so blessed to have you as my mother.

Additionally, I would like to thank our family pets: Sadie, Kitty Kitty, and Bean for filling my heart with so much love and joy. I know you three will never read this, however, you deserve your own section of thanks.

Lastly, I would like to thank Auburn for being the best home-away-from-home these past three years. You will forever have a piece of my heart.

It is with immense love, gratitude, and the loudest War Eagle, that I proudly present my thesis.

Table of Contents

List of Tables

List of Figures

Introduction

Global change is increasing ocean temperature

Anthropogenic climate change has devastating global impacts. Global greenhouse gas emissions continue to rise at unprecedented rates, resulting in a sharp increase in mass mortality events of species (Preston & Jones, 2006), irreversible loss of terrestrial, marine, and freshwater ecosystems (IPCC, 2023), and increases in extreme weather and storms (Brierley & Kingsford, 2009; IPCC, 2023). Humans are also not immune to climate challenges, with approximately 3.5 billion people living in regions highly vulnerable to climate change, and millions of people now exposed to food and water insecurity resulting from changing conditions (IPCC, 2023). Additionally, global temperature is rising due to greenhouse gas emissions, leading to warming of both marine and terrestrial ecosystems (IPCC, 2023). If we continue our current global emissions trend, conditions will only worsen, resulting in irreversible ecosystem loss and species extinction across the globe.

The ocean acts as a buffer to increases in both greenhouse gases and temperature (Reid et al., 2010) through absorbing approximately 93% of the extra energy produced from greenhouse gas emissions (Poloczanska et al., 2016). This buffering, however, has severe negative consequences for the ocean, with the absorption of extra energy resulting in increases in sea surface temperatures (SST) (Reid et al., 2010). Increases in SST have many long-term consequences, including impacts on heat transport (Reid et al., 2010), ocean circulation (Wilson et al., 2016), stratification (Sharples et al., 2013), and thermal expansion, leading to sea level rise (Reid et al., 2010). Increases in SST also has devastating effects on marine organisms, through altering dispersal pathways (Wilson et al., 2016), species range shifts (Brierley & Kingsford, 2009), and species invasion and extinctions (Brierley & Kingsford, 2009; Goldsmit et al., 2020).

Under current SST warming conditions, organisms may migrate to regions within their thermal tolerance to seek relief from warmer waters (Hastings et al., 2020; Sunday et al., 2012), resulting in poleward shift of species distribution, particularly in larval organisms, fish, invertebrates, and phytoplankton and zooplankton (Beaugrand et al., 2008; Hastings et al., 2020; Perry et al., 2005; Pitois & Fox, 2006).

Marine heatwaves are increasing due to global change

Climate change is also increasing the intensity, frequency, and duration of marine heatwaves (Frölicher et al., 2018; Shanks et al., 2020) with devastating long-term ecological and economic consequences. Marine heatwaves (MHWs) are periods of increased sea surface temperatures lasting weeks to months and can encompass thousands of kilometers of the ocean (Frölicher et al., 2018; Laufkötter et al., 2020). Specifically, a warming period is classified as a MHW when water temperatures exceed the 90^{th} percentile (of the 30-year historical baseline period) for five or more days (Hobday et al., 2016). Since the early twentieth century, the average occurrences of MHW days have nearly doubled (Oliver et al., 2018; Scannell et al., 2020), and this number is projected to continue to rise (Oliver et al., 2018).

Recently, MHWs have impacted regions of the Mediterranean, western Australia, the northwest Atlantic, and the northeast Pacific (Shanks et al., 2020). In the northeast Pacific, a MHW dubbed “The Blob” was a warming event lasting from 2013-2016, and more recently, a MHW lasting from 2019-2020 (dubbed “Blob 2.0”) plagued the same region (Amaya et al., 2020; Oliver et al., 2018; Scannell et al., 2020) and had devastating ecological consequences (K. E. Smith et al., 2023). This region of the ocean is becoming a hot spot for persistent MHW

events due to long-term warming resulting from anthropogenic greenhouse gas emissions (Laufkötter et al., 2020).

MHW events have severe impacts on marine ecosystems (Laufkötter et al., 2020), like kelp forests (Filbee-Dexter et al., 2020), coral reefs (Mellin et al., 2019) and sea grass beds (Strydom et al., 2020), and negatively influence marine organisms through increased mortality (Cavole et al., 2016; K. E. Smith et al., 2023), changes in species distributions and abundance (Smale et al., 2019), shifts in biodiversity (Laufkötter et al., 2020), and altered reproduction and recruitment of marine taxa (Shanks et al., 2020). For example, a fallout of the 2013-2016 Blob MHW resulted in significantly reduced or total reproductive failure across five taxa, including over dozens of marine invertebrates, and have devastated local marine populations (Shanks et al., 2020; K. E. Smith et al., 2023). Prolonged warming also contributes to low primary productivity, (Di Lorenzo & Mantua, 2016) and an increase in harmful algal blooms (HAB) (McCabe et al., 2016), leading to the closure of many important shellfish and crab fisheries (Di Lorenzo & Mantua, 2016; McCabe et al., 2016). It is projected that the economic cost of individual MHWs exceed $800 million in direct losses and more than $3.1 billion in indirect losses of ecosystem services (K. E. Smith et al., 2021).

Marine heatwaves are contributing to disease outbreaks in the ocean

Climate change can increase the likelihood of disease outbreak in the ocean (Burge et al., 2014), resulting from temperature increase (Harvell et al., 2019), pollution (Lafferty et al., 2004), and increased stress through habitat degradation (Kim et al., 2005; Lafferty et al., 2004). Under normal conditions, the rate of disease spread in the ocean is two orders of magnitude faster than

in terrestrial systems (McCallum et al., 2003), and this rate of disease spread is exasperated under increased temperatures (Burge et al., 2014).

Environmental shifts can cause a change in host-pathogen interactions (Burge et al., 2014), making organisms more susceptible to disease (Harvell et al., 1999). Disease outbreak can alter marine habitats through altering trophic interactions and community structures (Burge et al., 2014), specifically if the disease targets keystone predators or foundational species (Groner et al., 2016). Climate-related marine diseases are being observed for finfish (Couch & Fournie, 1993), corals (Randall & Van Woesik, 2015), sea stars (Miner et al., 2018), and even humans (Burge et al., 2014). Under elevated temperatures, marine pathogens like *Vibrio sp.*, sea star wasting disease, and coral black band disease thrive (Byers, 2020). Given the impact of sea surface temperature on ecosystems and diseases, it is important to understand how organisms respond to protect themselves when exposed to these new, stressful conditions.

Organisms must respond to a changing ocean

When exposed to challenging conditions, organismal response is critical to the success of both the individual and the species. Benthic marine invertebrates are particularly sensitive to changes to environmental conditions, specifically when faced with elevated temperature conditions (Vaquer-Sunyer & Duarte, 2011). Since benthic organisms are unable to quickly relocate (or relocate at all) to more favorable environments when conditions become stressful, they must either adjust to their new environment, or face mortality (Rivetti et al., 2014). Additionally, benthic marine invertebrates are primarily broadcast spawners (Marshall & Bolton, 2007) with their embryos developing as pelagic larvae and are subjected to the will of the currents (Pechenik, 1999; Pineda et al., 2012). Therefore, offspring can settle and metamorphose in environments different than their parents (Pineda et al., 2012). Development is a particularly

sensitive time for organisms, and especially so for larval marine invertebrates, as they face multiple stressors in the water column (Pechenik, 1999; Pineda et al., 2012). Therefore, they must have mechanisms in order to respond to these new challenges, or else face declines in population (Pechenik, 1999).

One way organisms are able to respond to variation in environmental condition is through the process of phenotypic plasticity, which is the ability of a single genotype to exhibit multiple phenotypes (West-Eberhard, 1989; Whitman & Agrawal, 2009). This plastic response is critical, especially when environmental variability occurs over a relatively short duration (Padilla & Savedo, 2013). Marine organisms are an excellent model to study phenotypic plasticity, as a wide range of traits (morphological, behavioral, chemical, and physiological), have been shown to produce a plastic response (Padilla & Savedo, 2013), particularly in response to fluctuating environmental conditions (Hadfield & Strathmann, 1996).

Epigenetic modifications assist in gene expression

When faced with adverse environmental conditions, marine organisms are capable of undergoing a variety of epigenetic modifications to better equip themselves, and their offspring, for success and survival in this new environment. Epigenetics is the change in gene expression without changing the underlying genetic sequence (Deans & Maggert, 2015), with the three types of epigenetic modifications consisting of DNA methylation (Singal & Ginder, 1999), histone modifications (Bannister & Kouzarides, 2011), and RNA-mediated regulation of gene expression (Holoch & Moazed, 2015). DNA methylation is the most studied of the epigenetic modifications (Beal et al., 2020), and involves the addition of a methyl group to the carbon 5 position of a cytosine ring (Singal & Ginder, 1999). There is variation in DNA methylation

patterns and functions between vertebrates and invertebrates (Feng et al., 2010; Suzuki et al., 2007; Zemach et al., 2010), however in invertebrates, DNA methylation is presented in a "mosaic" pattern (Suzuki et al., 2007) and is critical for gene expression (Moore et al., 2013). It is unknown how dynamic DNA methylation is throughout early developmental stages; additionally, it is important to understand natural variation occurring in DNA methylation patterns between individuals and developmental timepoints before we can fully understand how environmental stressors are resulting in variations.

Robust immune response buffers impact of marine pathogens

When faced with increased exposure to marine pathogens, marine organisms must have a defense mechanism to protect themselves, and these organisms rely on their immune systems as a first line of defense against disease. Immune responses can be divided into two branches – an innate immune response and an adaptive immune response. The innate immune system is more basal than the adaptive immune system and involves physical barriers as well as specific cell types to respond to a pathogen (Anaya et al., 2013). The adaptive immune system involves a series of primary lymphocytes with memory to recognize potential pathogens and launch a cell-mediated immune response (Kurtz, 2004; Pancer & Cooper, 2006). Most marine invertebrates contain an innate immune system and lack an adaptive immune response, however jawless vertebrates and vertebrates contain both an innate and an adaptive immune response (L. C. Smith, 2010). An innate immune system relies on self/nonself recognition where it launches a defensive attack to eliminate the invader and can also destroy its own damaged and diseased cells (Mydlarz et al., 2006).

Echinoderms are important marine organisms

Echinoderms (meaning “spiny skinned”) are a group of marine invertebrate deuterostomes characterized by a pentaradial symmetric adult body plan (Arnone et al., 2015). The approximate 6,500 living species that make up the phylum Echinodermata are divided into five classes; Crinoidea (feather stars), Asteroidea (sea stars), Ophiuroidea (brittle stars), Echinoidea (sea urchins), and Holothuroidea (sea cucumbers) (Alvarado & Cortés, 2009; Arnone et al., 2015), and are exclusively found in marine environments (Uthicke et al., 2009). Echinoderms contain a water vascular system used for circulation and locomotion (Arnone et al., 2015), and a exoskeleton containing spines to protect from predators. Echinoderms are found in all climatic zones, from rocky intertidal, to abyssal depths, to the frigid arctic (Arnone et al., 2015) and play a critical role in their ecosystem, with many considered keystone species (Uthicke et al., 2009).

Most echinoderms are broadcast spawners, meaning fertilization occurs externally in the water column, although there are some instances of echinoderms “brooding” (Arnone et al., 2015). Depending on the species, larvae are either planktotrophic (feeding) or lecithotrophic (non-feeding) (Arnone et al., 2015; Montgomery et al., 2017; Raff & Byrne, 2006; Strathmann, 1971). Planktotrophic larvae are usually derived from smaller, nutrient-poor eggs, and have prolonged periods of development where they must ingest food to survive and complete development (Allen & Pernet, 2007). Lecithotrophic larvae, however, originate from comparatively larger, energy-rich eggs, and do not need to consume food during their shorter larval periods (Allen & Pernet, 2007). During development, planktotrophic larvae, specifically certain sea urchin species, have an open gut which they use to filter food from their environment.

However, because of their open gut, other particulates and pathogens also enter their gut necessitating the larval immune response.

Echinoderms possess a robust innate immune system used to protect themselves from various marine pathogens (Hibino et al., 2006). Specifically, the immune system in larval sea urchins have been relatively well studied and characterized (Rast et al., 2006). There are five morphologically distinct cells that are critical for an immune response in sea urchin larvae; pigment cells, globular cells, filopodial cells, ovoid cells, and amoeboid cells (Ho et al., 2016). Pigment cells are red, mesenchymal cells, that get their red coloration from Echinochrome A (Ho et al., 2016). Pigment cells resemble adult red spherical cells in adults, which are critical for wound healing and activating an immune response (Ho et al., 2016). When exposed to marine pathogen *Vibrio diazotrophicus*, each immune cell type exhibits a robust response, with pigment cells and amoeboid cells migrating to the source of the pathogen, and filopodial cells acting to phagocytize foreign bodies (Ho et al., 2016). Although much has been discovered regarding larval and adult immune systems in the sea urchin, there has been limited work addressing the influence that adverse environmental conditions have on the formation of immune cells, and how additional environmental stressors impact immune function and response.

Study system and thesis goals

The California Current System (CCS) is a diverse and economically important region of the Pacific Ocean. The CCS stretches from Baja California, Mexico to Vancouver, Canada, where it is divided into three regions, the Northern, Central, and Southern region (Checkley & Barth, 2009), and is extremely productive due to it being a wind-driven upwelling zone (Checkley & Barth, 2009; Kämpf & Chapman, 2016). This upwelling pulls cold, nutrient rich waters to the surface due to the movement of ocean currents (Kämpf & Chapman, 2016) making

this region extremely biodiverse (Closek et al., 2019; Reese & Brodeur, 2006). However, the CCS is facing ecological challenges, and it has been the center of multiple MHWs (the Blob and Blob 2.0) throughout most of the 2010s. Therefore, research is needed to understand how marine organisms found within this environment are responding to these adverse conditions.

The purple sea urchin, *Strongylocentrotus purpuatus,* is a broadcast-spawning marine invertebrate found within the CCS (Tegner & Dayton, 1981; Zhadan et al., 2021). They are intense grazers, primarily feeding on giant kelp *Macrocystis pyrifera* (Tegner & Dayton, 1981), but are able to consume other macroalgae species when giant kelp is limited or otherwise unavailable (Foster et al., 2015). The purple sea urchin is predominantly preyed upon by the California sheep-head fish, spiny lobsters, and sea otters (Pearse, 2006; Tegner & Dayton, 1981), and is a keystone species in the CCS.

Purple sea urchins have a biphasic life-cycle, where they spend early development as planktotrophic larvae in the water column, and then metamorphose into benthic adults, where they remain for the duration of their life (Bosch et al., 1987). This synchronous development has been well annotated, making this organism an excellent model for not only epigenetic work, but for development and immunological research as well. Additionally, as one of the first organisms to have its entire genome sequenced, (Harris & Eddy, 2015; Sodergren et al., 2006), this has accelerated the research possibilities of this model organism.

The overall goals of my thesis are to (1) identify how marine heatwaves impact the morphology and immune cell development of *S. purpuratus* larvae through the quantification of their pigment cells and morphological measurements and (2) identify how DNA methylation patterns change throughout key developmental stages in *S. purpuratus* under ambient developmental conditions, while categorizing the influence that genotype has on these patterns.

Previous studies have identified how marine heatwave conditions impact body morphology of various echinoderms (Leach & Hofmann, 2023; Minuti et al., 2022; Strader et al., 2022), but this is the first study to quantify variation in their immune cells resulting from heat stress conditions. Additionally, to successfully quantify the impact that elevated temperature conditions have on DNA methylation patterns of the purple sea urchin (particularly throughout key developmental stages), we first must understand the natural variation occurring in methylation during development. Previous research has categorized DNA methylation in the purple sea urchin during a subset of early development stages (Xu et al., 2019), however this is the first study to encompass all major life history stages of purple sea urchin development, as well as identifying the influence that genotype has on each of these stages.

Chapter 1
Temperature influences immune cell development and body length in purple sea urchin larvae

Introduction

Marine heatwaves (MHWs) are increasing in frequency and intensity due to global change (Frölicher et al., 2018; Hobday et al., 2016), and are characterized by periods of elevated sea surface temperatures that last for weeks to months and can span thousands of kilometers (Frölicher et al., 2018). MHW events can have catastrophic impacts on marine habitats, notably coral reef ecosystems (Fordyce et al., 2019) and kelp forests (Smale et al., 2019); and can have drastic impacts on marine communities through species range shifts (Sanford et al., 2019) decreases in productivity (Whitney, 2015), altered food webs (Smith et al. 2021), and mass mortality events (Hoegh-Guldberg and Bruno, 2010; Laufkötter et al., 2020). MHW events are particularly stressful to benthic marine organisms, which are often unable to relocate to more favorable environments. As a result, during MHW events, benthic marine organisms must either have mechanisms by which to acclimate to their new environment via phenotypic plasticity, or face potential mortality (Snell-Rood et al., 2018; West-Eberhard, 2003).

The increased prevalence of MHWs has magnified disease prevalence in the ocean (Burge et al., 2014; Rubio-Portillo et al., 2015). Elevated ocean temperatures can increase disease transmission, host susceptibility, pathogen survival, and development rates (Harvell et al., 2002), which can threaten biodiversity and survivability of marine organisms. There is also a positive correlation between growth rates of marine bacteria and fungi and increased temperature (Harvell, 2002). For example, increased temperature leads to a higher susceptibility of white band disease in reef-building corals (Bruno et al., 2007; Burge et al., 2014; Heron et al., 2010), where the incidence of white band disease in *Acropora palmata* increases when median sea

surface temperatures are ≥28.5˚C (Randall et al., 2015). Although a limited number of mechanistic studies have been performed, two hypotheses for these observations have been proposed. First, that warmer waters relax the over-wintering dormancy of pathogenic microbes, resulting in a higher infection rate. Alternatively, it is possible that persistent heat induces a host stress response that suppresses immune system functions (Randall et al. 2015).

High temperatures have also been implicated in the recent increased disease prevalence of sea star wasting disease (SSWD), which affects at least twenty species of sea stars off the west coast of North America (Bates et al., 2009; Eisenlord et al., 2016; Kohl et al., 2016; Miner et al., 2018). This disease has the potential to drastically impact community composition through local extinction events (Montecino-Latorre et al. 2016) and has led to trophic cascades resulting in kelp barrens and altered population structures (Schultz et al. 2016). In cooler water temperatures, SSWD progression slows but still resulted in mortality events, indicating that if elevated temperatures do subside, SSWD infections persist (Kohl et al. 2016). Since MHWs are projected to increase in intensity and severity over the coming years (Frölicher et al., 2018; Hobday et al., 2016), disease prevalence and host susceptibility will continue to plague marine organisms leading to potentially irreversible damage in marine ecosystems. Here, we examine the consequences of marine heatwaves on the immune system development in another echinoderm species: the purple sea urchin (*Strongylocentrotus purpuratus*).

Strongylocentrotus purpuratus is an ecologically and economically important herbivore that inhabits the California Current System, which stretches from Baja California, Mexico to British Columbia, Canada (Pearse, 2006, Checkley & Barth, 2009, Manier & Palumbi, 2008). *S. purpuratus* are broadcast spawners with a biphasic life cycle that includes a long-lived planktotrophic larval stage that enables larvae to travel hundreds of kilometers on ocean currents

(Okamoto et al., 2020; Pearse, 2006). During this long pelagic stage, *S. purpuratus* larvae can experience drastically different temperatures and environmental conditions than those of their parents. Thus, larvae exhibit the capacity to acclimate to variable environments (Gray, 2013; Puisay et al., 2018). It has been shown that elevated temperatures increase both growth and development rate in sea urchin larvae (Fujisawa' & Shigei, 1990; O'Connor et al., 2007; Wong & Hofmann, 2020). Furthermore, temperatures experienced during early development has been shown to greatly influence survival in various tropical and temperate sea urchin species (Byrne et al. 2009, O'Connor et. al 2007, Sewell & Young 1999). Therefore, it is important to understand if and how temperatures experienced during early embryogenesis influence the development of the immune system, which may subsequently affect survival later in ontogeny.

The purple sea urchin has a sophisticated and complex innate immune system (Smith, 2012) composed of several specialized immune cell types that mediate pathogen responses in both the adult and larval life stages (Rast et al. 2006; Smith et al., 2006). In *S. purpuratus*, larval immune cells are derived from mesenchymal cells that are specified in early embryogenesis during the mid-blastula stage (Hobday et al., 2016; Solek et al., 2013). These include pigment cells, which, in uninfected animals, are primarily localize to the larval ectoderm, with concentrations on the tips of the arms and the apical end of the larvae (Ho et al., 2016). Resting pigment cells exhibit a stellate morphology. However, when exposed to certain strains of bacteria, pigment cells become active, change shape, and migrate to the site of infection (Ho et al., 2016, Smith et al., 2008).

Here, we identified how variation in developmental temperature impacts the morphology and immune cell development of *S. purpuratus* larvae. Specifically, we examined whether developmental temperatures, genotype, or both impacted the plasticity of larval body size and

immune response through the quantification of pigment cells. We find that larvae reared in elevated temperature were larger and had more pigment cells than those reared in ambient temperature. We also found that genotype influences pigment cell count, with significant variation in pigment cell counts between crosses, however no genotypic effect was found on overall body length. These results suggest that *S. purpuratus* larvae exhibit phenotypic plasticity in response to developmental temperature, not only in overall morphology, but also in immune system development. Since marine heatwaves are not projected to cease in duration or intensity in the near future (Frölicher et al., 2018; Hobday et al., 2016), and coincide with increases in marine diseases, (Burge et al., 2014; Rubio-Portillo et al., 2015) these results highlight that phenotypic plasticity in immune cell development may enable *S. purpuratus* larvae to persist during periods of prolonged heat stress.

Methods

Conditioning of adult urchins

Adult *S. purpuratus* were collected off the coast of Santa Barbara, California by SCUBA in October 2021 (SBC LTER permit = California Department of Fish and Wildlife Scientific Collecting permit #SC-9228) and were transported to a saltwater tank facility at Auburn University, where animals were housed in an 85-gallon aquarium. Animals were maintained in artificial seawater (Instant Ocean; 14˚C; salinity = 30 ppt). Temperature and salinity were monitored daily using an Apollo IV DT304 Digital Temperature Logger (UEI) and an ATC refractometer, while water chemistry was tested weekly using respective API test kits (API Saltwater Aquarium Master Test Kit). Adults were fed excess frozen kelp (*Macrocystis pyrifera*)

once a week and a 20% water change occurred two days after feeding to help stabilize water chemistry. Adults were acclimated to these conditions for three months prior to spawning.

Spawning of adults and culturing of larvae

Adults were selected at random for spawning, which occurred in two rounds. Spawning was induced by an injection of 0.53 M KCl into the coelomic cavity. Sperm was collected dry and remained on ice until activation. Eggs were collected in 0.22 μm-filtered artificial sea water (FASW) at 30 ppt salinity and 14˚C temperature. Gamete compatibility between individuals was assayed by checking the fertilization success (>90%) between different male/female pairs. For the first round of spawning, individual crosses were generated using one dam (Dam 1) and two sires (Sire 1 and 2). For the second round of spawning (which occurred two weeks later), individual crosses were established using a different set of adults, with two dams (Dam 2 and Dam 3) and one sire (Sire 3). Each spawning resulted in two unique genetic crosses, (4 total) from three males and three females. Fertilization occurred in ambient (14˚C) FASW. Fertilized embryos from each cross were divided into two different developmental temperatures: ambient (14˚C) and elevated (18˚C), each with two replicate cultures (Figure 1.1). Embryos were cultured in 4-liter vessels of FASW with stirring rotors at 20 rpm and a density of 10 embryos/μL (approximately 30,000 embryos per culture vessel).

Early life-history sampling

Larval cultures were maintained for six days, and partial (1/3 volume) water changes were performed at 3 days post fertilization (dpf) to maintain water quality. Offspring were collected at pluteus stage (6 dpf) to quantify variation in body length and pigment cell count between larvae developed in elevated versus ambient conditions. Pluteus larvae at both

temperatures were fully developed by 6 dpf, not necessitating difference in timing samples due to developmental delay. Approximately 600 larvae from each culture vessel were sampled for morphological analysis, preserved in 10% aqueous buffered zinc formalin (Z-Fix; Anatech, Ltd.), and stored at 4˚C.

Egg and early embryo morphology imaging and analysis

Unfertilized eggs from each spawned female were also preserved in Z-Fix (approximately 600 eggs per female, collected in triplicate). Individual eggs (n=30 per female per triplicate) were selected at random and photographed using a Canon Rebel X digital camera and calibrated with a scale micrometer. Images were processed in FIJI (National Institute of Health, USA). Average egg diameter was determined by taking the average of three independent diameter measurements at angles 0˚, 45˚, and 90˚ to account for potential irregularities in egg shape. To avoid bias in slide preps containing multiple eggs, each egg was randomly assigned a number and a random number generator was used to choose the egg to be measured.

Pluteus morphology imaging and analysis

To measure pigment cell number and overall body length, 3D images were taken of the pluteus larvae (N=10 per cross replicate) from a series of Z-stacks taken with a Zeiss Axio Observer 7 microscope and Zen Imaging Software (Zen 3.0 blue edition). Each image consisted of 50 slices of an interval of 0.57 µm. Images were processed using FIJI (National Institute of Health, USA) using the "Cell Counter" plugin (De Vos, 2001) (Supplemental Figure 1.1). Pigment cells were counted manually. To accurately measure larval morphology, the X, Y, and Z coordinates were collected from each pre- and post-oral arm, as well as the apical end. The

formula $\sqrt{(x_2 - x_1)^2 + (y_2 - y_1)^2 + (z_2 - z_1)^2}$ was used to calculate larval body length. Pre- and post-oral arm length was averaged for each individual larva.

Statistical Analysis

All statistical analysis was conducted in R (version 4.1.2). All tests were run with a linear mixed effect model using the R data packages *lme4* (Linear Mixed-Effects Models using 'Eigen' and S4, version 1.1-34; (Bates et al., 2015)) and *afex* (Analysis of Factorial Experiments, version 1.3; (Singmann et al., 2023). Models used to test if female identity played a role in egg size, included fixed effects of female and random effect of egg ID. To identify variation in pigment cell count, a linear mixed effect regression model (lmer) was used with developmental treatment and genetic combination used as fixed effects, while individual culture vessel used as a random effect. There was also an interaction between genetic combination and treatment that was accounted for as a fixed effect in the model. Additional, separate lmer models were run to identify variation in pigment cell count due to maternal and paternal effects. The function *emmeans* (Estimated Marginal Means, aka Least-Squares Means, version 1.8.8, (Lenth, R. 2023)). was used to extrapolate individual comparisons. The same model structure was used for identifying variation in preoral body length as well as postoral body length due to developmental temperature. Finally, a linear model using the *lm* package in R (lm: Fitting Linear Models, R stats package, version 4.2.3) was used to identify correlations between larval body length and pigment cell counts, with developmental temperature used as the fixed effect. Separate correlations were performed to compare preoral body length and pigment cell count and for postoral body length and pigment cell count. Significance was defined as $p<0.05$.

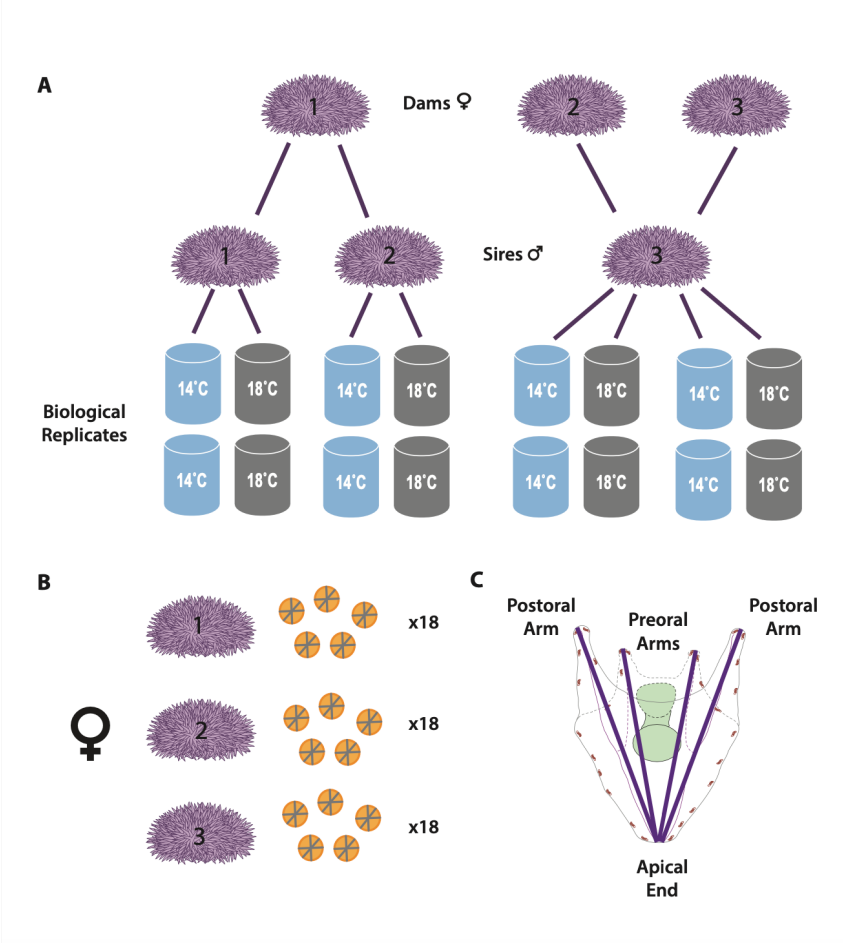

Figure 1.1: Experimental design investigating the role of developmental temperature on larval immune phenotypes. **(A)** Gametes were collected from three adult sires and three adult dams and crossed as shown. Cultures of fertilized embryos were divided and grown in either ambient (14˚C, depicted in blue) or elevated (18˚C, depicted in grey) temperatures. Each culture condition was replicated twice for a total of two biological replicates per cross and condition. **(B)** A subsample of unfertilized eggs was saved for morphological analysis from each dam. Three measurements (0˚, 45˚, and 90˚) were taken per egg (n=90 per dam) and averaged together to get one diameter value per egg. **(C)** Pluteus samples (6dpf) were measured from each genetic cross and each developmental condition. Preoral and postoral body length was measured (denoted with purple lines) and pigment cells were counted.

Results

Egg diameter varies among dams

Unfertilized eggs were collected from the three dams prior to fertilization to quantify variation in egg size among females. Results indicate that the three females produced eggs of significantly different sizes (Figure 1.2). Dam 1 had the largest egg diameter with an average diameter of 94.17 µm (0.869, SE), while dam 2 and dam 3 had an average egg diameter of 88.93 µm (0.876, SE) and 88.13 µm (0.869, SE), respectively. There was a significant difference in egg diameter from eggs originating from dam 1 and dam 2 (p_{lmer} =0.0119, Figure 1.2, Supplemental Table 1.2) and dam 1 and dam 3 (p_{lmer} =0.0066, Figure 1.2, Supplemental Table 1.2). However, there was no significant difference in egg diameter between dam 2 and dam 3 (p_{lmer} =0.8317, Figure 1.2, Supplemental Table 1.2). A size difference of ~6 µm in egg diameter can correspond to up to a 14% difference in volume, showing that the smallest variation in egg diameter can have sizable variation in total volume.

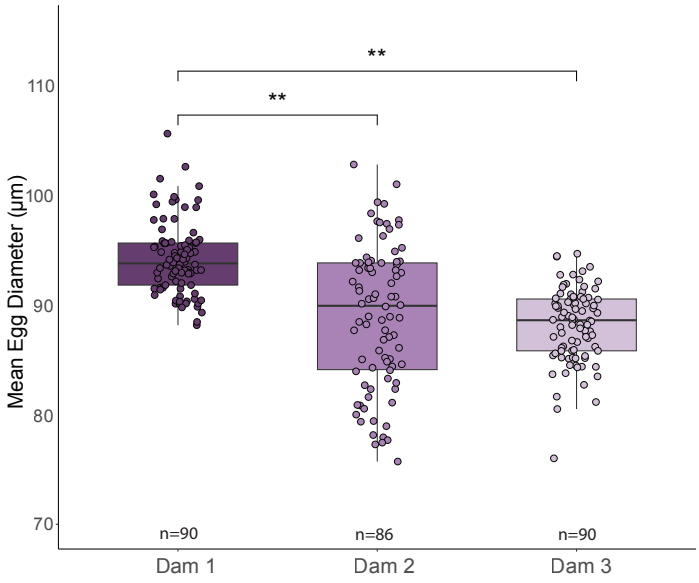

Figure 1.2: Egg diameter varies among dams. Each egg was measured three times using orthogonal planes and averaged per egg. Significant differences in egg size between individual dams are denoted with asterisks ($p_{lmer} < 0.01$).

Larvae grow larger when cultured in higher temperatures

To determine the effects of genotype and temperature on preoral and postoral larval body length, we generated four distinct genetic crosses from six adult sea urchins. Fertilized embryos were grown at either ambient (14˚C) or elevated (18˚C) temperatures (Figure 1.1). Larval morphology was monitored until the 4-armed pluteus stage (6 dpf). At this stage, larvae have fully developed their gut and are able to appropriately feed and swim, further, immune cells have developed by this stage (Ho et al., 2016).

Results indicate that preoral body length was significantly affected by temperature during embryogenesis. Pluteus larvae that developed in elevated temperatures were significantly larger (average length of 272 ± 12.0 µm, 95% CI) than larvae grown in ambient temperatures (average length of 252 ± 11.0 µm, 95% CI; p_{lmer}=0.0211, Figure 1.3A). To investigate the possibility maternal effects influence preoral body length, we identified variation in overall preoral body

length in larvae produced by the three dams. Independent of temperature conditions, we found that there was no significant difference in preoral body length based on dam (Figure 1.3C, Supplemental Table 1.3G,I). To identify if paternal effects drive preoral body length, we quantified preoral body length based on sire. We found that there were no significant paternal effects on preoral body length, independent of temperature treatment (Figure 1.3D, Supplemental Table 1.3H,I). Finally, no significant genotypic effect was observed on preoral body length when comparing our four genetic crosses (Supplemental Table 1.3F,I, Figure 1.3B).

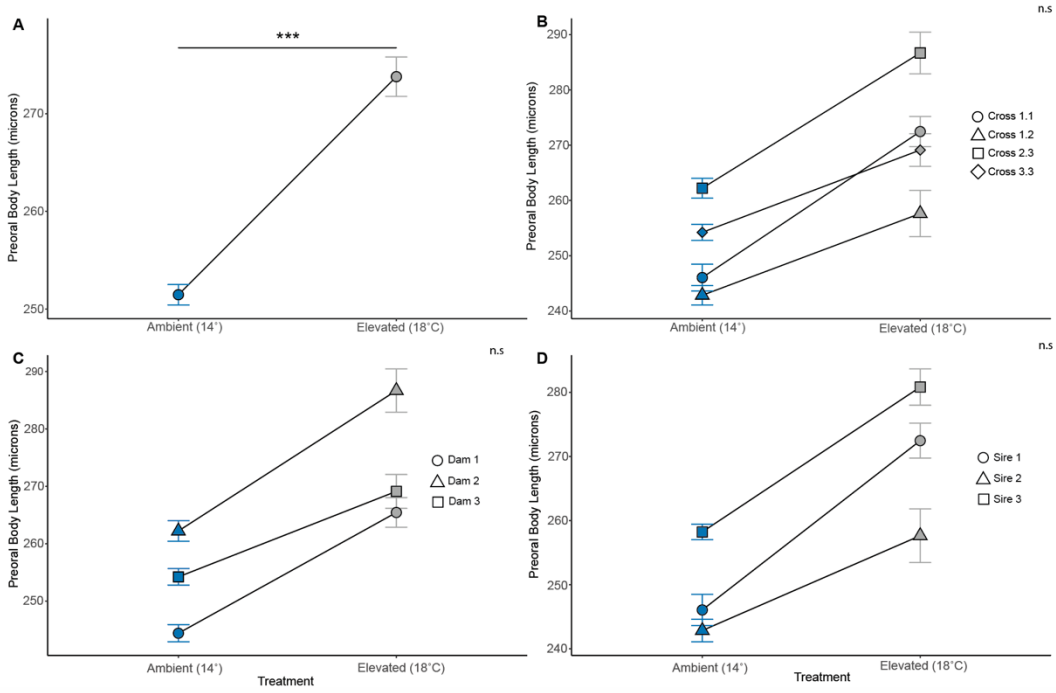

Figure 1.3: Embryos developed at elevated temperature exhibit longer pre-oral body lengths **(A)** Difference in preoral body length between larvae which developed in ambient temperatures compared to larvae which developed in elevated temperatures (lmer, p=0.0211). **(B)** Differences in preoral body length between dams. **(C)** Preoral body length differences between genetic crosses. **(D)** Differences in preoral body length between sires. Asterisks denote significant differences (lmer, $p<0.05$).

Postoral body length was significantly affected by temperature during embryogenesis. The postoral body lengths of pluteus larvae that developed in elevated temperatures were

significantly larger than larvae that developed in ambient temperature conditions (p_{lmer}=0.0324, Figure 1.4A). The average postoral body length of larvae cultured in elevated temperatures was an average of 276 µm (±14 µm, 95% CI); growing in ambient temperatures resulted in an average postoral body length of 253 µm (± 13.0 µm, 95% CI). We investigated potential influences of maternal or paternal effects on postoral body length and found that no significant differences independent of temperature conditions (Figure 1.4C, Supplemental Table 1.3L,M; Figure 1.4D, Supplemental Table 1.3K,M).

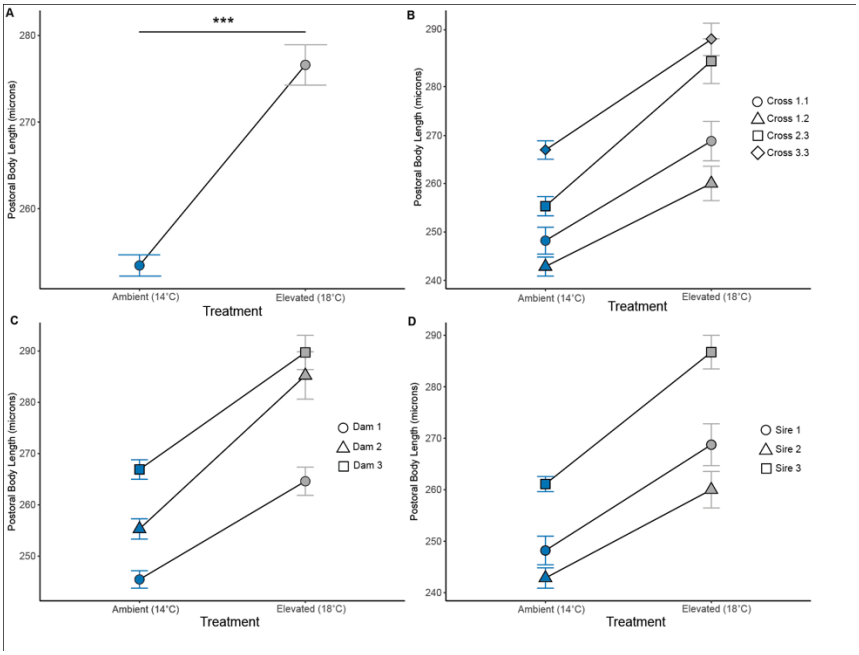

Figure 1.4: Embryos developed at elevated temperatures exhibit longer postoral body lengths. (A) Differences in postoral body length between larvae developed in ambient temperatures compared to larvae which developed in elevated temperatures (p_{lmer}=0.0324). (B) Postoral body length differences between genetic crosses. (C) Differences in postoral body length between dams. (D) Differences in postoral body length between sires. Blue colored shapes indicate ambient conditions (14˚C) while grey colored shapes indicate elevated conditions (18˚C). Asterisks denote significance differences (p_{lmer}<0.001 = ***)

Higher temperatures during embryogenesis impact pigment cell development

In addition to identifying the effect of temperature and genotype on larval body length, we characterized how developmental temperature influences immune cell development. Given their importance in responding to immune challenge and distinctive morphology (Buckley & Rast, 2019; Ho et al., 2016), we enumerated pigment cells in each larva. On average, larvae reared in at 18°C had more pigment cells than larvae grown in ambient conditions (p_{lmer}=0.000431, Figure 1.5A).

To determine the role of genotype on pigment cell development, we investigated the role of genotype, maternal and paternal effects on pigment cell development. Analyses of individual crosses revealed that genotype did not significantly influence pigment cell numbers for larvae reared in ambient temperature conditions but was an important factor in larvae reared in elevated temperatures (Figure 1.5B). Specifically, in elevated conditions, larvae from cross 1.1 in had ~25 more pigment cells than larvae from cross 3.3 (p_{lmer}= 0.0046), or cross 2.3 (p_{lmer}= 0.0034, Figure 1.5B, Supplemental Table 1.3B,C). However, the same crosses did not have significantly different pigment cell numbers under ambient conditions. Similarly, larvae from cross 1.2 had on average 16 more pigment cells when grown at 18°C compared to the cross 2.3 (p_{lmer}=0.0169) and ~20 more pigment cells than cross 3.3 (p_{lmer}= 0.0169, Figure 1.5B, Supplemental Table 1.3B,C).

To address if maternal effects drive pigment cell variation among individuals, we compared larvae produced from the three dams used. At ambient temperature, no significant variation was observed (Figure 1.5C, Supplemental Table 1.3C). However, we found that dam played a significant role in pigment cell count. In elevated temperatures, larvae produced from dam 1 had on average 19 more pigment cells than larvae produced from dam 2 (p_{lmer}=0.0009, Figure 1.5C, Supplemental Table 1.3C,D) or dam 3 (p_{lmer}=0.0015, Figure 1.5C, Supplemental Table 1.3C,D). Additionally, there was no significant difference in pigment cell count between

dam 2 and dam 3 under elevated temperature (p_{lmer} =0.72, Figure 1.5C, Supplemental Table 1.3C,D). Similarly to the maternal effects, we found that under ambient treatment conditions, there were no significant differences between pigment cell count based on sire (Figure 1.5D, Supplemental Table 1.3C,E), while effects were evident under elevated temperature. Larvae produced from sire 1 had on average 23 more pigment cells compared to larvae produced from sire 3 in under elevated temperature (p_{lmer} =0.0001, Figure 1.5D, Supplemental Table 1.3C,E). Additionally in the elevated temperature, larvae produced from sire 2 had significantly more pigment cells compared to larvae produced from sire 3 (p_{lmer} =0.001, Figure 1.5D, Supplemental Table 1.3C,E). Although there no significant different in pigment cell count between larvae produced from sire 1 and sire 2 in the elevated temperature, (p_{lmer} =0.3454, Figure 1.5D, Supplemental Table 1.3C,E).

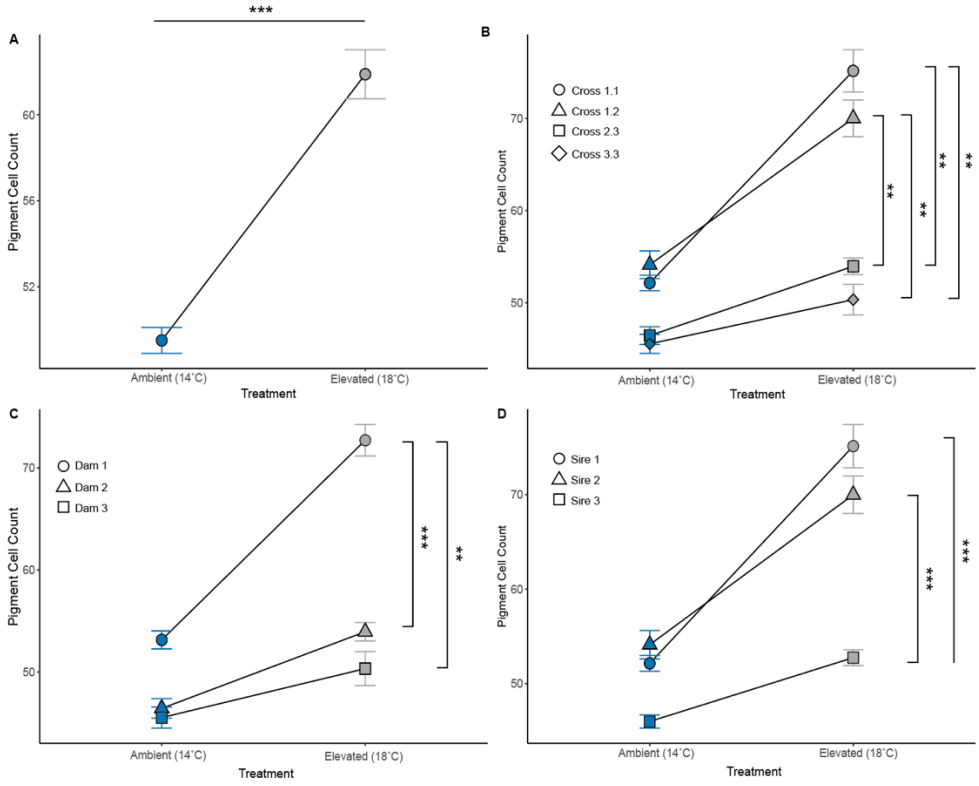

Figure 1.5: Variation in immune pigment cells among genetic crosses reared in different developmental temperature. (A) Differences in pigment cell count between larvae developed in ambient and elevated temperatures (B) Differences in pigment cell count between unique genetic crosses. C) Differences in pigment cell count between dams. D) Differences in pigment cell count between sires. Asterisks denote significant differences (p_{lmer} <0.001 = ***; p_{lmer} <0.01 = **; p_{lmer} <0.05 =*)

We found that being a larger larva did not correspond to having more pigment cells. Correlations between postoral body length and pigment cell count in ambient temperature, showed a negative, statistically significant, small correlation between the two variables (r^2 = 0.041, 95% CI [-0.30, -0.05], p = 0.007, Figure 1.6). Additionally, under elevated temperature, we identified a negative, statistically not significant correlation between pigment cell count and postoral body length (r^2 = 0.023, 95% CI [-0.30, 1.93e-03], p =0.053, Figure 1.6).

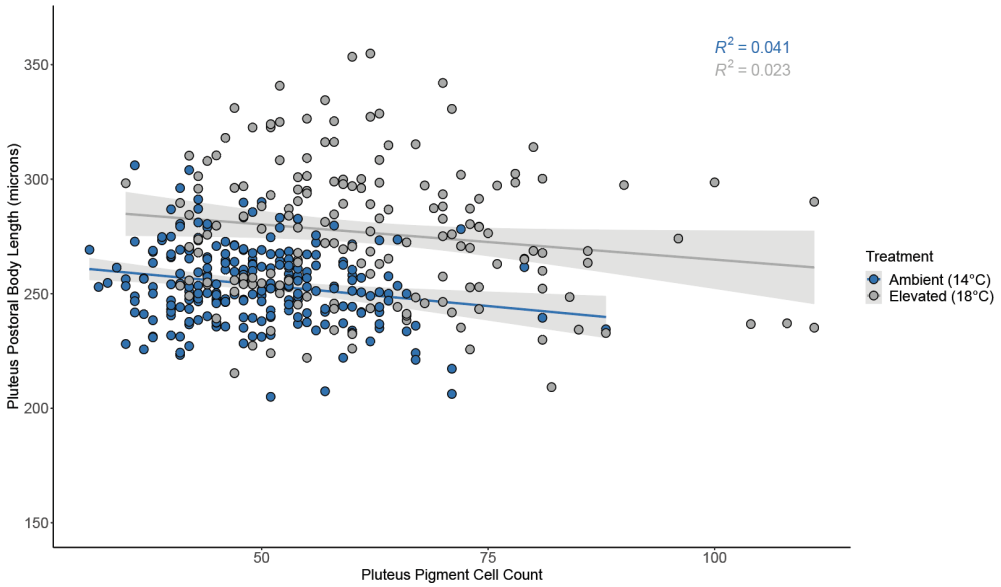

Figure 1.6: Relationship between pigment cell count and postoral body length. Blue circles denote larvae reared in the ambient (14˚C) treatment. Dark grey circles indicate larvae reared in the elevated (18˚C) treatment. Light grey shading indicates standard error.

Lastly, we quantified if egg size influenced larval postoral body length and pigment cell count for larvae in both developmental treatments. We found no significant correlation between egg diameter and postoral body length for larvae reared in ambient conditions for dam 1 (r^2 = 0.0041, p = 0.629, Figure 1.7A), for dam 2 (r^2 = 0.0029, p = 0.684, Figure 1.7A) or for dam 3 (r^2 = 0.002, p = 0.734, Figure 1.7A), or for larvae reared in elevated conditions for dam 1 (r^2 = 0.18, p = 0.333, Figure 1.8A), or for dam 2 (r^2 =6.4e-06, p = 0.989, Figure 1.8A). However, we did identify a positive, significant, correlation between egg diameter and postoral body length for dam 3 in elevated conditions (r^2 = 0.21, p = 0.012, Figure 1.8A). Similarly, there was no significant correlation between pigment cell count and egg diameter for samples reared in ambient conditions originating from dam 1 (r^2 = 0.00099, p = 0.811, Figure 1.7B) or from dam 2 (r^2 = 0.0018, p = 0.746, Figure 1.7B). However, there is a positive, statistically significant

correlation between pigment cell count and egg diameter between samples reared in ambient conditions originating from dam 3 ($r^2 = 0.083$, $p = 0.025$, Figure 1.7B). For samples reared in the elevated conditions, we found no significant correlation between egg diameter and pigment cell count between samples reared in elevated conditions originating from dam 1 ($r^2 = 0.0029$, $p = 0.779$, Figure 1.8B), dam 2 ($r^2 = 0.0045$, $p = 0.725$, Figure 1.8B), or dam 3 ($r^2 = 3.9e\text{-}06$, $p = 0.992$, Figure 1.8B).

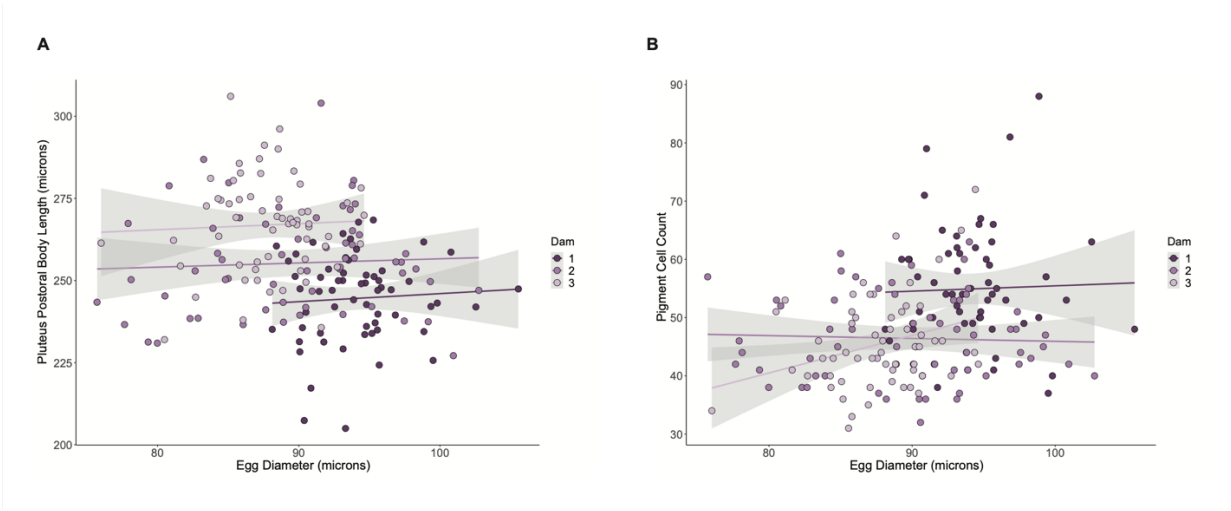

Figure 1.7: Relationship between egg diameter and larval postoral body length **(A)** or pigment cell count **(B)** for larvae developed in ambient (14˚C) temperature.

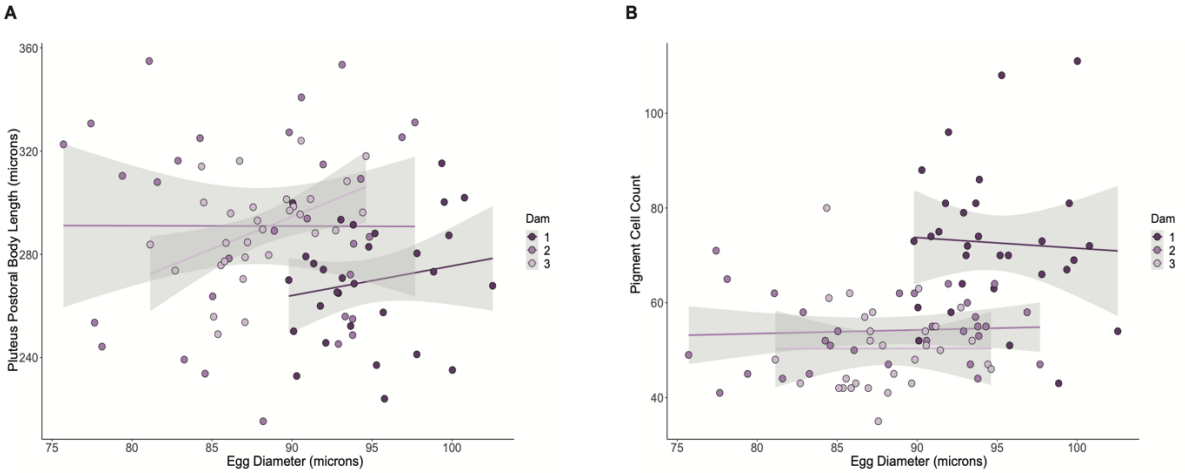

Figure 1.8: Relationship between egg diameter and larval postoral body length (A) or pigment cell count (B) for larvae developed in elevated (18˚C) temperature.

Discussion

We investigated the role of temperature on body length and immune cell development in S. *purpuratus* larvae and found that elevated temperature during embryogenesis resulted in larvae that were larger with an increased number of pigment cells. This variation results from the environment as well as genotype but was not driven by differences in maternal provisioning, as inferred through differences in egg size. Overall, these results suggest that environmental temperature is a primary driver of plasticity during development.

Egg diameter varies among dams

In broadcast spawning marine organisms, egg size is one of the most important factors contributing not only to fertilization success, but to larval growth, development, and ultimately survival (Moran & Mcalister, 2009). Although egg size is critical for species success, this phenotype is extremely variable not only between species, but also between individuals.

Therefore, in the context of how early developmental environments shape phenotypes, it is important to have a comprehensive understanding of when variation is occurring, and what could be driving these differences. In this study, we found significant variation in egg diameter between dams. However, when identifying if variation in egg size influences larval postoral body length or pigment cell count, we found that there was no correlation between egg size on those two factors, regardless of developmental condition. This suggests that maternal provisioning, which we infer from unfertilized egg size, was not a contributing factor shaping later larval size and immune capabilities.

Intraspecific variation in egg size is not uncommon in broadcasting spawning marine organisms (Emlet & Hoegh-Guldberg, 1997; Levitan, 2000, 2006; Marshall et al., 2000; Mcedward & Carson, 1987) and can be driven by environmental conditions, genetic variation, or stochastic developmental processes (Moran & Mcalister, 2009; Vogt et al., 2008). The temperature experienced by dams during oogenesis can influence the size of the egg produced (Moran & Mcalister, 2009), but likely did not cause the sizes differences in the eggs observed here, as the urchins used for this experiment were collected during the same dive event at the same site and were housed in the same common garden aquarium for three-months prior to spawning. However, we are unaware of the conditions they experienced in the wild, and their previous spawning history, which would most likely have a stronger influence on their egg size. Additionally, although adult urchins did not spawn during the three-month acclimation period, their previous spawning history in the wild is unknown and could have contributed to the intraspecific variation observed in our study.

Maternal age can also influence the size of the egg produced, with egg size decreasing with advanced maternal age in marine invertebrates (Ito, 1997; Moran & Mcalister, 2009; Qian

& Chia, 1992). Since our adult urchins were collected from the wild, we are unable to know for certain their age and if this is contributing to the variation we observed in egg diameter. Maternal size can also contribute to overall egg size, with previous research showing that larger mothers produce larger eggs (George, 1994; Marshall et al., 2000; Moran & Mcalister, 2009). This may be attributed to maternal size as an indicator of the number of resources a mother can provide to reproduction (George, 1994). However, we saw the opposite trend with our dams. Although they were randomly selected at the time of spawning, dam 1 was the smallest with a diameter of 56 cm and a height of 35 cm and produced the largest eggs, while dam 3 was the largest with a diameter of 73 cm and a height of 38 cm and produced the smallest eggs (Supplemental Table 1.4). Although our observations differ from what is reported in the literature, there may be additional factors that interact with maternal size that may contribute to the variation in egg diameter observed.

For broadcast-spawning marine invertebrates, the entire maternal nutritive contribution from the mother to their offspring is provided in the egg, potentially making larger eggs better equipped to handle developmental stressors (Mcedward & Carson, 1987). Additionally, studies also show that larger eggs are larger targets for sperm, which is extremely beneficial for broadcast-spawning organisms, especially in sperm-limited conditions (Levitan, 1996; Marshall & Keough, 2007). However, being too large of an egg can be detrimental compared to smaller eggs when there is a high male density, as polyspermy in large eggs occurs more frequently, as it takes a moment for the blocks of polyspermy to take effect (Marshall & Keough, 2007). Therefore, it is important to be the right egg size for the density of males in the environment. After fertilization, egg size can greatly influence larval growth, development, and survival, with

larvae derived from larger eggs having an increased survival rate (Emlet, 1995; Levitan, 2000; Marshall & Keough, 2007).

Developmental temperature influences overall body length in larval sea urchins

The environment an individual develops in has a monumental influence over their success and survival as an adult (Gray, 2013; Marshall et al., 2003; Shima & Findlay, 2002). When faced with adverse environmental conditions, organisms can either relocate to a more favorable site, adjust to their new environment, or perish. However, larval marine organisms are often subjected to the will of the currents, therefore, are unable to relocate to more favorable environments. Temperature is one of the most influential environmental conditions impacting larval development, so understanding how developmental temperature shapes larval phenotypes is extremely important in understanding how organisms respond to changing environments (Byrne, 2011; Byrne & Przeslawski, 2013; O'Connor et al., 2007; Pechenik, 1984). We found that pluteus length which developed in elevated temperatures were significantly larger than those which developed in the ambient temperatures. These results indicate that larval sea urchins are phenotypically plastic to variation in temperature in their developmental environment. Larval plasticity resulting from variation in developmental temperatures has been well documented in marine invertebrate larvae (Byrne, 2011; Byrne & Przeslawski, 2013; González-Ortegón & Giménez, 2014; O'Connor et al., 2007; Reitzel et al., 2004), specifically in echinoderms (Byrne & Przeslawski, 2013; Dellatorre & Manahan, 2023; Hoegh-Guldberg & Pearse, 1995; Karelitz et al., 2020; Leach & Hofmann, 2023; Wangensteen et al., 2013; Wong & Hofmann, 2020).

The mechanistic driver that influences increased larval body length when exposed to elevated temperature is an increase in metabolic activity (Byrne, 2011; Sardi et al., 2023;

Somero, 2002). Water temperature increases in biological activity and biochemical reactions resulting from elevated temperatures, thus altering metabolic rates (Dellatorre & Manahan, 2023; Sin et al., 2019). In *S. purpuratus*, higher temperatures have been shown to increase not only metabolic rates, but also overall body length, specifically an increase in arm length (Dellatorre & Manahan, 2023). Longer arms increase food acquisition rates, which can help compensate for increased energy needs (Dellatorre & Manahan, 2023). Additionally, amino acid transporters in the larval arms of purple sea urchins are critical for metabolic processes like osmoregulation, nutrition, and protein synthesis, and are in direct contact with seawater, aiding in the transport of nutrients from the environment (Christensen et al., 1965; Meyer & Manahan, 2009).

In addition to morphological and metabolic changes resulting from variation in temperature, there are ecological consequences of planktonic larvae developing in increased water temperatures. Increased developmental temperatures has been shown to impact planktonic larval duration, leading to a shorter amount of time larvae are in the water column (Byrne, 2011; O'Connor et al., 2007). A shorter planktonic larval duration has many benefits to larvae, including a decreased predation rate, a faster settlement rate, and a higher survival rate (Allen, 2008; Byrne et al., 2011; Hare & Cowen, 1997). For instance, under elevated temperature conditions, planktonic larvae of *Rhopaloeides odorabile*, a common sponge found in the Great Barrier Reef, settled 36 hours faster than those at ambient temperature conditions (Whalan et al., 2008). Shortened planktonic larval duration can limits genetic connectivity between populations since larvae are not traversing the water column for as long (O'Connor, 2007). Additionally, since predators prefer smaller echinoderm larvae, an increase in larger larvae can influence the predator-prey dynamics of marine food webs (Allen, 2008). Since marine heat waves (MHWs) are projected to increase in intensity and duration (Frölicher et al., 2018; Hobday et al., 2016),

and SST are rising at alarming rates (Hoegh-Guldberg et al., 2014), our results reveal challenges larval marine organisms, specifically *S. purpuratus* larvae, will face.

Lastly, to identify whether genotype influences postoral body length during larval development, we generated four distinct genetic crosses and exposed embryos from each cross to both experimental conditions until they reached 6dpf (Figure 1.1). We found that genotype did not significantly impact postoral body length, regardless of developmental temperature. These results indicate developmental temperature is the primary driver of plasticity in larval length. Our results differ, however, from previous research investigating genotypic effects influencing larval morphometrics. In Leach & Hofmann (2023), researchers found that both paternal identity, and the interaction between paternal identity and larval environment, significantly impacted larval arm length in *S. purpuratus* larvae. Although they investigated an earlier echinopluteus larval stage than we investigated here, these results indicate that there could be additional drivers influencing larval plasticity in a stressful environment, or that genotypic effects in larval body morphometrics are prominent at earlier developmental stages and may cease in later larval life.

Developmental temperature and genotype influence pigment cell count in larval sea urchins

Planktonic larvae are directly exposed to the open ocean and need to protect themselves against pathogens in their environment in order to reach adulthood. However, changes in environmental conditions can lead to an increase in pathogens (Cohen et al., 2018; Vezzulli et al., 2013), thus necessitating a robust immune system to respond to these pathogens. We identified significant variation in pigment cell counts in larvae reared in elevated temperatures compared to larvae from ambient conditions, with larvae exposed to increased temperatures having significantly more pigment cells on average compared to the ambient larvae. These results

demonstrate that larval sea urchins can alter their immune response after prolonged exposure to adverse environmental conditions to better protect themselves from harmful pathogens they may face in their stressful environment.

Echinoid larvae are the only larvae in the phylum which possess pigment cells, making them an interesting model to investigate environmental impacts on immune response (Spurrell et al., 2023). Pigment cells are often used as an indicator for immune response in purple sea urchin larvae due to their red coloration, which makes cells easily quantifiable and traceable in transparent larvae. Further, there is a well characterized suite of genes that code for their formation and expression, including polyketide synthase 1 (*SpPks1*), flavin-dependent monooxygenase 3 (*SpFmo3*) and macrophage migration inhibitory factor 5 (*SpMif5*) (Spurrell et al., 2023). These pigment cell precursor genes are first expressed in the blastula stage of development and are expressed throughout development (Spurrell et al., 2023). Although we know the genes responsible for pigment cells, and how cells respond to pathogenic stressors, this is the first study to our knowledge that examines how these cells respond to altered environmental conditions. Future work should examine if the genes which regulate pigment cells production are modulated during embryogenesis in different environmental conditions to produce increased pigment cells observed here or if the pigment cells themselves divide as a response to exposure to elevated temperatures.

While our study is the first to connect temperature with immune responses in larval sea urchins, ocean temperatures have dramatic impact immune responses in other marine invertebrates. In prolonged exposure to elevated water temperatures, abalones exhibit compromised antibacterial responses and increases in antiviral activity, indicating a potential trade-off in immune response because of heat stress (Dang et al., 2012). Additionally, larval

lobsters (*H. americanus*) under elevated temperature conditions have higher total hemocyte concentration, an indicator of the innate immune response (Harrington et al., 2019). These results highlight the ability of marine organisms to adjust their immune system to better defend themselves against pathogens.

Similarly to the *S. purpuratus* larval stage, the adult purple sea urchin has a complex immune repertoire responsive to environmental change, with coelomocytes serving as the foundation for the adult immune system (Barela Hudgell et al., 2022; Matranga et al., 2000, 2005; Rast et al., 2006; L. C. Smith et al., 2006). In response to temperature stress, coelomocytes increase in concentration (particularly red sphere cells and phagocytes) (Branco et al., 2012) as well as overexpress 70 kDa heat shock protein (Matranga et al., 2000). In some cases, sea urchin coelomocytes are even used as bioindicators of environmental stressor (Matranga et al., 2000). These results show that immune cells in adult sea urchins are eluding a response when exposed to environmental stressors, which we also observe after developing in elevated temperature conditions.

Lastly, we found that genotype contributed significantly to variation in pigment cell count, but only for larvae that developed at higher temperatures, suggestive of genotype x environment (GxE) interactions. Similarly, in *Crassostrea gigas* larvae there is a significant interaction between environmental temperature, host genotype, and pathogen genotype (GxGxE), with disease resistance occurring in the warmer experimental conditions (Wendling et al., 2017). These results indicate that there is a strong genetic basis to the development of the immune system, and that larvae exposed to elevated temperature have the potential to be better equipped to handle environmental pathogens. Larvae in our experiment were grown in filtered (0.2 micron) ASW and were not knowingly exposed to a bacterial pathogen. Thus, the responses

observed are likely based on factors that we controlled for (i.e. temperature and genotype), and not as a response to an additional pathogen.

We find that *S. purpuratus* larvae are phenotypically plastic in response to developmental temperature, specifically in how larvae develop critical immune cells and thus their ability to defend against potential pathogens and diseases. Since marine heatwaves are projected to increase in duration and intensity in the near future (Frölicher et al., 2018; Hobday et al., 2016), coinciding with increases in marine diseases, (Burge et al., 2014; Rubio-Portillo et al., 2015) these results highlight that phenotypic plasticity in immune cell development may enable *S. purpuratus* larvae to persist during periods of prolonged heat stress.

Supplementary Materials

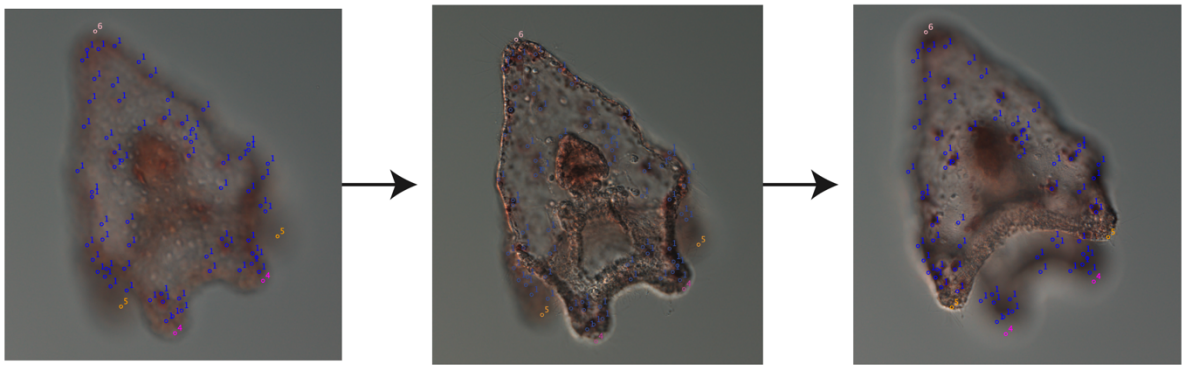

Supplemental Figure 1.1: Quantifying pigment cell count and preoral and postoral body length in pluteus larvae. A total of 50 slices per individual Z-stack were taken to quantify pigment cell count and body length. All points were added by hand using Cell Counter in FIJI. The three images represent three of the 50 slices analyzed, and points remained between each slice to prevent pigment cells from being counted multiple times. Blue dots denoted with "1" represent pigment cells, magenta dots denoted with "4" represent preoral arms, golden dots denoted with "5" represent postoral arms, and pink dots denoted with "6" represent the apical end.

Supplemental Table 1.1: Spreadsheet containing pigment cell counts and preoral and postoral body length measurements for all individuals sampled. This spreadsheet is included as a separate excel file and can be found at: https://github.com/emw0083/thesis_documents/.

Supplemental Table 1.2: Spreadsheet containing egg diameter measurements for each of the three dams sampled. This spreadsheet is included as a separate excel file and can be found at: https://github.com/emw0083/thesis_documents.

Supplemental Table 1.3: Model results for all statistical tests. **(A):** Egg size variability between the three dams sampled **(B):** Pigment cell mean values for each genetic cross **(C):** Significance values of pigment cell counts **(D):** Emmean for dam pigment cell count **I:** Emmean for sire pigment cells count **(F):** Emmean for genetic cross preoral body length **(G):** Emmean for dam preoral body length **(H):** Emmean for sire preoral body length **(I):** Significance values for preoral body length values **(J):** Emmean for postoral body length for genetic **(K):** Emmean for sire postoral body length **(L):** Emmean for dam for postoral body length **(M):** Significance values for postoral body length

(A): Egg size variability between the three dams sampled

Test	df	t-value	p-value
Dam 1 vs Dam 2	6.03	4.304	**0.0119**
Dam 1 vs. Dam 3	5.94	4.909	**0.0066**
Dam 2 vs. Dam 3	6.03	0.589	0.8317

(B): Pigment cell mean values for genetic cross

Treatment	Cross	emmean	SE	df	lower CL	upper CL
Ambient (14˚C)	1.1	52	2.66	6.71	45.7	58.4
Ambient (14˚C)	1.2	54.1	2.65	6.62	47.8	60.5
Ambient (14˚C)	2.3	46.6	2.65	6.57	40.1	52.8
Ambient (14˚C)	3.3	45.5	2.65	6.57	39.2	51.9
Elevated (18˚C)	1.1	75.2	2.78	7.95	68.7	81.6
Elevated (18˚C)	1.2	69.8	2.83	8.47	63.3	76.2
Elevated (18˚C)	2.3	54	2.65	6.57	47.6	60.3
Elevated (18˚C)	3.3	50.3	3.75	6.57	41.4	59.3

I: Significance values of pigment cell counts

Treatment	Test	SE	df	t-value	p-value
Ambient (14˚C)	Cross 1.1 vs Cross 1.2	3.76	6.66	-0.556	0.9417
Ambient (14˚C)	Cross 1.1 vs Cross 2.3	3.76	6.64	1.491	0.4918
Ambient (14˚C)	Cross 1.1 vs Cross 3.3	3.76	6.64	1.731	0.3798
Ambient (14˚C)	Cross 1.2 vs Cross 2.3	3.75	6.59	2.052	0.2607
Ambient (14˚C)	Cross 1.2 vs Cross 3.3	3.75	6.59	2.292	0.1938
Ambient (14˚C)	Cross 2.3 vs Cross 3.3	3.75	6.57	0.24	0.9946
Ambient (14˚C)	Dam 1 vs Dam 2	3.25	8.4	2.047	0.1602

Ambient (14˚C)	Dam 1 vs Dam 3	3.25	8.4	2.324	0.1067
Ambient (14˚C)	Dam 2 vs Dam 3	3.75	8.36	0.24	0.9688
Ambient (14˚C)	Sire 1 vs Sire 2	3.46	8.65	-0.602	0.8227
Ambient (14˚C)	Sire 1 vs Sire 3	3	8.65	2.02	0.165
Ambient (14˚C)	Sire 2 vs Sire 3	2.99	8.55	2.723	0.0578
Elevated (18˚C)	Cross 1.1 vs Cross 1.2	3.96	8.21	1.362	0.5531
Elevated (18˚C)	Cross 1.1 vs Cross 2.3	3.84	7.24	5.521	**0.0034**
Elevated (18˚C)	Cross 1.1 vs Cross 3.3	4.67	7.02	5.319	**0.0046**
Elevated (18˚C)	Cross 1.2 vs Cross 2.3	3.87	7.49	4.08	**0.0169**
Elevated (18˚C)	Cross 1.2 vs Cross 3.3	4.69	7.18	4.138	**0.0169**
Elevated (18˚C)	Cross 2.3 vs Cross 3.3	4.59	6.57	0.788	0.8576
Elevated (18˚C)	Dam 1 vs Dam 2	3.31	9.02	5.604	**0.0009**
Elevated (18˚C)	Dam 1 vs Dam 3	4.24	8.75	5.228	**0.0015**
Elevated (18˚C)	Dam 2 vs Dam 3	4.59	8.36	0.788	0.72
Elevated (18˚C)	Sire 1 vs Sire 2	3.68	11.03	1.461	0.3454
Elevated (18˚C)	Sire 1 vs Sire 3	3.26	9.76	6.879	**0.0001**
Elevated (18˚C)	Sire 2 vs Sire 3	3.3	10.21	5.165	**0.001**

(D): Emmean for dam pigment cell count

Treatment	**Dam**	**emmean**	**SE**	**df**	**lower CL**	**upper CL**
Ambient (14˚C)	1	53.1	1.88	8.48	48.8	57.4
Ambient (14˚C)	2	46.4	2.65	8.36	40.4	52.5
Ambient (14˚C)	3	45.5	2.65	8.36	39.5	51.6

Elevated (18˚C)	1	72.5	1.98	10.43	68.1	76.9
Elevated (18˚C)	2	54	2.65	8.36	47.9	60
Elevated (18˚C)	3	50.3	3.75	8.36	41.8	58.9

I: Emmean for sire pigment cell count

Treatment	**Sire**	**emmean**	**SE**	**df**	**lower CL**	**upper CL**
Ambient (14˚C)	1	52	2.45	8.72	46.5	57.9
Ambient (14˚C)	2	54.1	2.44	8.57	48.6	59.7
Ambient (14˚C)	3	46	1.72	8.51	42	49.9
Elevated (18˚C)	1	75.2	2.58	10.64	69.5	80.8
Elevated (18˚C)	2	69.8	2.63	11.43	64	75.5
Elevated (18˚C)	3	52.7	1.99	8.51	48.2	57.3

(F): Emmean for genetic cross preoral body length

Treatment	**Genetic Cross**	**emmean**	**SE**	**df**	**lower CL**	**upper CL**
Ambient (14˚C)	1.1	246	11.6	6.96	219	274
Ambient (14˚C)	1.2	243	11.6	6.94	215	270
Ambient (14˚C)	2.3	262	11.6	6.93	235	290
Ambient (14˚C)	3.3	254	11.6	6.93	227	282
Elevated (18˚C)	1.1	272	11.7	7.13	245	300
Elevated (18˚C)	1.2	256	11.7	7.2	229	284

Elevated (18˚C)	2.3	287	11.6	6.93	259	314
Elevated (18˚C)	3.3	269	16.4	6.93	230	308

(G): Emmean for dam preoral body length

Treatment	Dam	emmean	SE	df	lower CL	upper CL
Ambient (14˚C)	1	244	7.73	8.91	227	262
Ambient (14˚C)	2	262	10.93	8.88	237	287
Ambient (14˚C)	3	254	10.93	8.88	229	279
Elevated (18˚C)	1	264	7.8	9.22	247	282
Elevated (18˚C)	2	287	1093	8.88	262	311
Elevated (18˚C)	3	269	15.45	8.88	234	304

(H): Emmean for sire preoral body length

Treatment	Sire	emmean	SE	df	lower CL	upper CL
Ambient (14˚C)	1	246	10.94	8.96	221	271
Ambient (14˚C)	2	243	10.93	8.93	218	268
Ambient (14˚C)	3	258	7.73	8.92	241	276
Elevated (18˚C)	1	272	11.01	9.21	248	297
Elevated (18˚C)	2	256	11.05	9.32	231	281
Elevated (18˚C)	3	281	8.92	8.92	261	301

(I): Significance values for preoral body length values

Treatment	Test	SE	df	t-value	p-value
Ambient (14˚C)	Cross 1.1 vs Cross 1.2	16.4	6.95	0.208	0.9965
Ambient (14˚C)	Cross 1.1 vs Cross 2.3	16.4	6.94	-0.98	0.7653
Ambient (14˚C)	Cross 1.1 vs Cross 3.3	16.4	6.94	-0.492	0.9584
Ambient (14˚C)	Cross 1.2 vs Cross 2.3	16.4	6.93	-1.188	0.6529
Ambient (14˚C)	Cross 1.2 vs Cross 3.3	16.4	6.93	-0.7	0.8939
Ambient (14˚C)	Cross 2.3 vs Cross 3.3	16.4	6.93	0.488	0.9594
Ambient (14˚C)	Dam 1 vs Dam 2	13.4	8.89	-1.328	0.4163
Ambient (14˚C)	Dam 1 vs Dam 3	13.4	8.89	-0.731	0.7523
Ambient (14˚C)	Dam 2 vs Dam 3	15.5	8.88	0.518	0.8649
Ambient (14˚C)	Sire 1 vs Sire 2	15.5	8.95	0.22	0.9737
Ambient (14˚C)	Sire 1 vs Sire 3	13.4	8.95	-0.901	0.653
Ambient (14˚C)	Sire 2 vs Sire 3	13.4	8.93	-1.156	0.5064
Elevated (18˚C)	Cross 1.1 vs Cross 1.2	16.5	7.17	0.985	0.7624
Elevated (18˚C)	Cross 1.1 vs Cross 2.3	16.5	7.03	-0.864	0.8231
Elevated (18˚C)	Cross 1.1 vs Cross 3.3	20.1	6.99	0.166	0.9982
Elevated (18˚C)	Cross 1.2 vs Cross 2.3	16.5	7.07	-1.851	0.3268
Elevated (18˚C)	Cross 1.2 vs Cross 3.3	20.1	7.02	-0.642	0.915
Elevated (18˚C)	Cross 2.3 vs Cross 3.3	20.1	6.93	0.874	0.8181
Elevated (18˚C)	Dam 1 vs Dam 2	13.4	8.99	-1.663	0.2705
Elevated (18˚C)	Dam 1 vs Dam 3	17.3	8.95	-0.276	0.9592
Elevated (18˚C)	Dam 2 vs Dam 3	18.9	8.88	0.928	0.6376

Elevated (18˚C)	Sire 1 vs Sire 2	15.6	9.26	1.043	0.5695
Elevated (18˚C)	Sire 1 vs Sire 3	14.2	9.09	-0.59	0.8288
Elevated (18˚C)	Sire 2 vs Sire 3	14.2	9.16	-1.735	0.2443

(J): Emmeans for postoral body length for genetic cross

Treatment	**Genetic Cross**	**emmean**	**SE**	**df**	**lower CL**	**upper CL**
Ambient (14˚C)	1.1	248	14.2	6.96	215	282
Ambient (14˚C)	1.2	243	14.2	6.94	209	76
Ambient (14˚C)	2.3	255	14.2	6.94	222	289
Ambient (14˚C)	3.3	267	14.2	6.94	233	301
Elevated (18˚C)	1.1	269	14.3	7.11	235	302
Elevated (18˚C)	1.2	259	14.3	7.17	225	292
Elevated (18˚C)	2.3	285	14.2	6.94	252	319
Elevated (18˚C)	3.3	290	20.1	6.94	242	337

(K): Emmean for sire postoral body length

Treatment	**Sire**	**emmean**	**SE**	**df**	**lower CL**	**upper CL**
Ambient (14˚C)	1	248	12.87	8.96	219	278
Ambient (14˚C)	2	243	12.86	8.93	214	272
Ambient (14˚C)	3	261	9.09	8.92	241	282
Elevated (18˚C)	1	269	12.95	9.2	240	298
Elevated (18˚C)	2	259	12.99	9.3	230	288

Elevated (18˚C)	3	287	10.5	8.92	263	311

(L): Emmeans for dam for postoral body length

Treatment	Dam	emmean	SE	df	lower CL	upper CL
Ambient (14˚C)	1	246	9.07	8.91	225	266
Ambient (14˚C)	2	255	12.82	8.89	226	284
Ambient (14˚C)	3	267	12.82	8.89	238	296
Elevated (18˚C)	1	264	9.15	9.21	243	284
Elevated (18˚C)	2	285	12.82	8.89	256	314
Elevated (18˚C)	3	290	18.13	8.89	249	331

(M): Significance values for postoral body length

Treatment	Test	SE	df	t-value	p-value
Ambient (14˚C)	Cross 1.1 vs Cross 1.2	20.1	6.95	0.279	0.9918
Ambient (14˚C)	Cross 1.1 vs Cross 2.3	20.1	6.95	-0.344	0.9848
Ambient (14˚C)	Cross 1.1 vs Cross 3.3	20.1	6.95	-0.921	0.7953
Ambient (14˚C)	Cross 1.2 vs Cross 2.3	20.1	6.94	-0.623	0.9215
Ambient (14˚C)	Cross 1.2 vs Cross 3.3	20.1	6.94	-1.2	0.6462
Ambient (14˚C)	Cross 2.3 vs Cross 3.3	20.1	6.94	-0.577	0.9359
Ambient (14˚C)	Dam 1 vs Dam 2	15.7	8.89	-0.62	0.8134
Ambient (14˚C)	Dam 1 vs Dam 3	15.7	8.89	-1.358	0.4014
Ambient (14˚C)	Dam 2 vs Dam 3	18.1	8.89	-0.64	0.8026

Ambient (14˚C)	Sire 1 vs Sire 2	18.2	8.95	0.308	0.9493
Ambient (14˚C)	Sire 1 vs Sire 3	15.8	8.95	-0.808	0.7079
Ambient (14˚C)	Sire 2 vs Sire 3	15.7	8.93	-1.164	0.5021
Elevated (18˚C)	Cross 1.1 vs Cross 1.2	20.3	7.14	0.494	0.9579
Elevated (18˚C)	Cross 1.1 vs Cross 2.3	20.2	7.02	-0.817	0.8448
Elevated (18˚C)	Cross 1.1 vs Cross 3.3	24.7	7	-0.85	0.8296
Elevated (18˚C)	Cross 1.2 vs Cross 2.3	20.2	7.06	-1.312	0.5842
Elevated (18˚C)	Cross 1.2 vs Cross 3.3	24.7	7.02	-1.255	0.6157
Elevated (18˚C)	Cross 2.3 vs Cross 3.3	24.6	6.94	-0.182	0.9976
Elevated (18˚C)	Dam 1 vs Dam 2	15.8	8.99	-1.363	0.3985
Elevated (18˚C)	Dam 1 vs Dam 3	20.3	8.95	-1.279	0.441
Elevated (18˚C)	Dam 2 vs Dam 3	22.2	8.89	-0.202	0.9777
Elevated (18˚C)	Sire 1 vs Sire 2	18.3	9.25	0.545	0.8513
Elevated (18˚C)	Sire 1 vs Sire 3	16.7	9.09	-1.079	0.5494
Elevated (18˚C)	Sire 2 vs Sire 3	16.7	9.15	-1.676	0.2651

Supplemental Table 1.4: Morphological measurements of the six adults used in this experiment.

Individual	Diameter	Height
Sire 1	72 cm	37 cm
Sire 2	56 cm	33 cm
Sire 3	64 cm	34 cm
Dam 1	56 cm	35 cm
Dam 2	70 cm	40 cm
Dam 3	73 cm	38 cm

Chapter 2
DNA methylation patterns vary throughout early development of *Strongylocentrotus purpuratus*

Introduction

The field of epigenetics is rapidly expanding across both vertebrate and invertebrate taxa. Epigenetics is the study of the mechanisms which alter gene expression without changing the DNA nucleotide sequence (A. Bird, 2002; Bossdorf et al., 2008). One of the most common and well-studied epigenetic mechanisms in eukaryotes is DNA methylation, which is the addition of a methyl group to the 5' portion of the cytosine ring (Singal & Ginder, 1999). This reaction is catalyzed by DNA methyltransferases (DNMTs) and occurs primarily in the CpG dinucleotide (5'-CG-3') (Singal & Ginder, 1999) while also providing an important toolkit for epigenetic regulations (Lyko, 2018). This CpG methylation can have major implications on gene expression, transcription, gene silencing, genomic imprinting, and embryogenesis (A. Bird, 2002; Hsieh, 1994; Jones, 2012; Suzuki & Bird, 2008; Xu et al., 2019) and can also influence phenotypic plasticity in organisms (Roberts & Gavery, 2012). Although CpG methylation is the most prominently identified methylation type, methylation can also occur at CHH sites or CHG sites, where the H is either adenine, thymine, or cytosine (Hearn et al., 2019). CHH and CHG methylation are more commonly found in plants, however they do occur in low levels in invertebrate and vertebrate organisms. (Dabe et al., 2015; Hearn et al., 2019; Ichiyanagi et al., 2013).

DNA methylation is considered to be evolutionarily ancient, however, there is great variation in methylation patterns between vertebrate and invertebrate organisms (Feng et al., 2010; Klughammer et al., 2023; Roberts & Gavery, 2012; Suzuki et al., 2007; Zemach et al.,

2010). Vertebrate genomes are more heavily methylated compared to invertebrate genomes, where approximately 70-80% of the genome is methylated in a phenomenon dubbed global methylation (Bird & Taggart, 1980; Roberts & Gavery, 2012). The minimal amount of the vertebrate genome that is not methylated is found in CpG-rich regions like CpG islands, often found near the promoter regions of genes (Feng et al., 2010; Roberts & Gavery, 2012).

Invertebrates have varying reduced levels of DNA methylation compared to their vertebrate counterparts. In invertebrates, the genomes either lack methylation, as seen in fruit flies and worms, or are methylated in a mosaic pattern, as seen in the sea anemone, honeybee, and sea urchins (Feng et al., 2010; Roberts & Gavery, 2012; Suzuki et al., 2007; Xu et al., 2019). Previous research found that for invertebrate deuterostomes, like the sea squirt and the sea urchin, that methylation levels are approximately 0.25-0.3 in the genome (Xu et al., 2019). In invertebrates, methylation predominately occurs in the form of gene body methylation (including methylation of exons and introns). Although its purpose is not as clear as it is for mammals, researchers propose that methylation in invertebrates contributes to regulation of transcription and can also mediate alternative splicing (Dixon & Matz, 2022; Feng et al., 2010; Hearn et al., 2019; Suzuki et al., 2007; Ying et al., 2022; Zemach et al., 2010). Gene body methylation has also been associated with various housekeeping genes in invertebrates, specifically HOX genes (Sarda et al., 2012; Suzuki & Bird, 2008).

There is growing interest in identifying if and how methylation patters change throughout fertilization and early development, specifically in invertebrate organisms. Previous work has identified changes in methylation patterns among various development timepoints in the pacific oyster (*Crassostrea gigas*) and identified the importance of DNA methylation for oyster development, as it influences gene expression (Riviere et al., 2013). Additionally, researchers

have identified variation in DNA methylation in the marbled crayfish (*Procambarus virginalis*) during its developmental stages and found that methylation levels increase throughout developmental stages and then decrease with age, with this methylation contributing heavily to phenotypic differences in genetically identical clutch-mates (Vogt, 2022).

Additional work has been done to elucidate if and how the parental methylome influences the methylation patterns of their offspring. In vertebrates, there are varying ideas as to whether DNA methylation patterns are inherited from parents, or if the methylome is reset after fertilization. Researchers have found that methylome reprogramming during embryogenesis does not occur in cnidarians or insects, but does begin to occur in deuterostomes like echinoderms, and then becomes even more prevalent in vertebrates (Xu et al., 2019). Additionally, researchers have uncovered that genome-wide demethylation is only identified in mammals and is not found in other vertebrates or invertebrates (Xu et al., 2019).

The purple sea urchin, *Strongylocentrotus purpuratus*, is an ecologically and economically important herbivore found in the California Current System, which stretches from Baja California, Mexico to British Columbia, Canada (Checkley & Barth, 2009; Manier & Palumbi, 2008; Pearse, 2006). *S. purpuratus* are broadcast spawning marine invertebrates, in which one spawning event can produce millions of offspring (Levitan, 1998). What makes this model an excellent system to study is that spawning can be easily induced in a laboratory setting, and the ability to establish distinct genetic crosses between adults makes genotyping experiments feasible. Additionally, *S. purpuratus* has a synchronous developmental timeline. Development of sea urchins are divided into three distinct periods – the embryonic period, planktonic period, and adult period (Formery et al., 2022). The embryonic period can be further divided into three subsequent periods – the cleavage period, the blastula period, and gastrulation period (Formery

et al., 2022). These periods are made up of various embryonic stages, with each embryonic stage taking approximately an hour to progress, until the gastrulation period which slows to approximately two hours a stage (Formery et al., 2022). The prism stage is the last stage of the embryonic period and occurs approximately three days post fertilization (dpf) (Adonin et al., 2021). The four-armed pluteus stage is reached approximately 5dpf (Adonin et al., 2021), and sea urchins remain in this planktonic pluteus period until metamorphosis (Formery et al., 2022), which occurs approximately ~50 dpf (Adonin et al., 2021). This synchronous developmental timeline makes sampling at specific timepoints feasible and reliable. Additionally, the annotated *S. purpuratus* reference genome (Sodergren et al., 2006) allows for genetic work, including DNA methylation, to be accomplished. In combination, this makes the purple sea urchin an excellent model for epigenetic research.

Enzymatic methyl-seq (EM-seq) is a new approach to methylome analysis. Traditional bisulfite sequencing treats sequences with sodium bisulfite, which converts unmethylated cytosines to uracils, leaving methylated cytosines intact. The uracils are then sequenced as thymines, leaving the only cytosines remaining methylated (Williams et al., 2019). This process is harsh on the DNA strands and can result in fragmentation and loss of DNA (Williams et al., 2019). EM-seq, however, uses the enzyme Apolipoprotein B mRNA editing enzyme subunit 3A (APOBEC3A) to deaminate cytosines to uracils, and Ten-eleven translocation (TET2) and an Oxidation Enhancer to protect the methyl group to prevent removal by APOBEC3A (Williams et al., 2019). This process results in an increased sensitivity of detection of CpGs and greater mapping efficiency compared to other methods resulting in a more accurate representation of the methylome (Feng et al., 2020; Williams et al., 2019). Although different, both methodologies produce the same end result, meaning that previously established bisulfite analysis pipelines can

be utilized to analyze EM-seq data. Using EM-seq to identify methylation profiles in the purple sea urchin at a single-base resolution will contribute to this growing literature base and will be crucial in helping to identify the evolution of DNA methylation and its changes between invertebrates and vertebrates.

Previous research has identified how DNA methylation patterns in the purple sea urchin change after exposure to various environmental stressors (Bogan et al., 2023; Strader et al., 2019, 2020), however, to better understand how their epigenome is changing in response to complex environmental conditions, we must first establish a baseline methylation profile to understand if the changes observed is the result of the external stressor, or if it is changes in methylation resulting from development that we are witnessing. Previous research has categorized methylation up to the gastrulation stage of development of the purple sea urchin (Xu et al., 2019), however methylation patterns of later developmental stages (prism and pluteus) and of adult cell types are still unknown.

The goal of this study Is to identify variation in DNA methylation patterns across three distinct genotypes over eight specific developmental stages of *S. purpuratus* offspring. We found that both genotype and developmental stage contribute significantly to methylation patterns in *S. purpuratus*. Specifically, methylation is primarily concentrated in the intergenic region of the gene body. We additionally identified gene-specific methylation differences between the three genotypes as well as across the eight developmental stages and found that genes responsible for methyltransferase activity and protein binding are differentially methylated. These results indicate that the purple sea urchin has a dynamic methylation profile throughout development, with genotypic influences.

Methods

Collection of Urchins

Adult *S. purpuratus* were hand-collected by SCUBA off the coast of Santa Barbara, California, USA and were transported to the saltwater tank facility at Auburn University, where animals were housed in an 85-gallon aquarium. All animals were maintained in artificial seawater at a temperature of 14˚C and salinity of 30ppt. Temperature and salinity were measured daily using Apollo IV DT304 Digital Temperature Logger (UEI) and an ATC refractometer, while water chemistry was tested weekly using respective API test kits (API Saltwater Aquarium Master Test Kit). Adults were fed excess frozen kelp (*Macrocystis pyrifera*) once a week, and a 20% water change occurred two days after feeding to help stabilize water chemistry.

Spawning of urchins and sample collection

Spawning was induced by an injection with 0.53M KCl into the coelomic fluid. Sperm was collected dry and remained on ice until activation. Oocytes were collected in 0.22 micron filtered artificial sea water (FASW) at 30 ppt salinity and gamete compatibility between individuals was assayed by checking the fertilization success (>90%). To account for genotypic effects on early methylation patterns, three distinct genetic crosses were established (here by referred to as “Cross 6”, “Cross 7”, and “Cross 8”). Early developmental stages (thirty-two cell, morula, and blastula) were cultured in beakers at approximately 40,000 embryos per beaker, and embryos for used for prism and pluteus collection were cultured in 4-liter buckets of FSW with stirring rotors at 20rpm and a density of 10 embryos/uL (approximately 25,000 embryos per culture vessel). Each culture vessel and beaker had a biological replicate. Oocytes and sperm were saved from each adult spawned to assess DNA methylation patterns. Additionally, after

spawning, a sample of tube feet from each of the nine adults were collected for DNA extraction to identify DNA methylation patterns in the adult tissue. Additional samples were collected at the thirty-two cell stage (7 hpf), morula stage (10 hpf), blastula stage (24 hpf), prism stage (3 dpf), and pluteus stage (8 dpf) for each of the three genetic crosses (Figure 2.1). Genomic DNA was extracted using an established CTAB extraction protocol (Strader et al., 2019), and quality and integrity of DNA was analyzed using gel electrophoresis and quantified on a Qubit fluorometer 3.0 (Life Technologies). Whole genome DNA methylation sequencing was performed using the EMSeq kit (NEB), following manufacturing instructions.

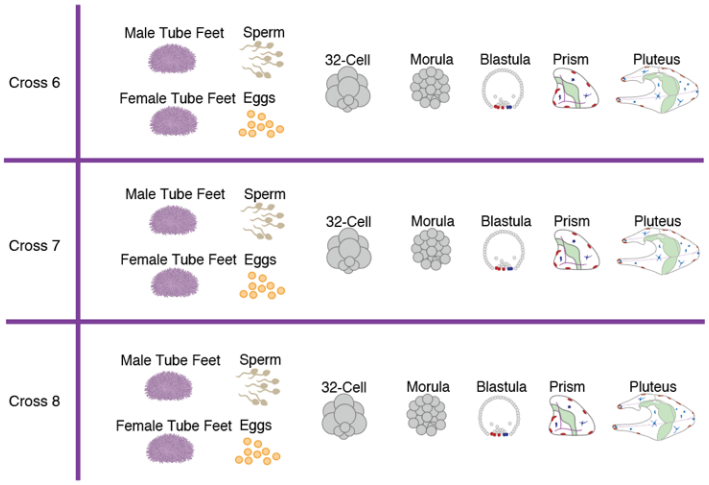

Figure 2.1: Table of all developmental stages and genetic crosses sampled for DNA methylation. Due to low conversion efficiency, oocytes from all three genetic crosses were removed from downstream analysis.

Sample Pre-processing

The Alabama Supercomputer was utilized for the initial analysis of sequencing files. Raw sequence files were visualized using FastQC (Andrews, 2010) to to assess read quality. Sequences were trimmed using Trim Galore! Version 0.6.6 (Krueger et al. 2021) which utilizes

cutadapt version 1.13 (Martin, 2022) to remove the adaptor sequences and short reads from the 3' end of sequences. Additionally, the first 10bp on the 5' end were clipped to avoid poor quality and biases, and a quality phred score of 20 was used. FastQC was rerun using the trimmed files to ensure sequences were removed and to assess trimmed read quality. The reference genome (*Stronglyocentrotus purpuratus* [v5.0]) (Sodergren et al., 2006) was converted for bisulfite alignments, and bisulfite converted trimmed reads were mapped against it using Bismark (v0.23.1) (Krueger & Andrews, 2011). Conversion efficiency was also calculated for each of the 27 individual sample. However, the conversion efficiency for the three oocyte samples (eg6, eg7, eg8) was below 90%, therefore, they were removed from subsequent analysis. Bismark deduplication was run to remove alignments in the same position in the genome. Methylation coverage files were produced using the bismark_methylation_extractor command, and bismark2report and bismark2summery were run to produce a graphical summary of the methylation data. All subsequent output files for this portion of the analysis can be found in Supplemental Table 2.1. The resulting coverage files were used for the remainder of the analysis.

Statistical analysis

Statistical analysis on resulting coverage files were completed using the program □*ethylKit* (Akalin et al., 2012) via Bioconductor (Gentleman et al., 2004) using R (version 4.2.1). Coverage files were filtered, and bases that had more than the 99.9th percentile of coverage or had coverage below 10X were discarded. Filtered samples were merged into one object which contained methylation information for the bases covered in all the 24 samples, which was used to identify correlations in methylation profiles across the samples using the *getCorrelation* command in methylKit (Akalin et al., 2012). Percent methylation per site for each

of the 24 samples was calculated using a built in methylKit command (*percMethylation*). Principle coordinate analysis (PCoA) was conducted using Manhattan distance using the *vegan* (Okasanen, F.J., et al. 2017), *ape* (Paradis and Schliep, 2019), and *adegenet* (Jombart, 2008) packages, and an ANOVA using *adonis2* was run to determine the proportion of variance in percent methylation explained by fixed factors (genotype and developmental stage). Additionally, the correlation of percent methylation between developmental stage and genotypes was visualized using a custom heatmap (*pheatmap version 1.0.12*).

Identifying differential methylation and associated genes

Differential methylation per CpG site (DMCpGs) was calculated using a logistic regression model using a q-value < 0.01 and a percent methylation difference larger than 25% (Akalin et al., 2012). Hypermethylated and hypomethylated bases were also identified. DMCpG calculation was run eleven independent times, once for each of the eight developmental stages (male tube feet, female tube feet, sperm, thirty-two cell, morula, blastula, prism, and pluteus) and for each of the three genetic crosses (Cross 6, Cross 7, Cross 8). Lastly, to determine in which genomic region the DMCpGs were occurring, these sites were annotated using NCBI's Reference Sequences *Strongylocentrotus purpuratus* genome (v.5.0) to identify if CpG sites were occurring in a promotor, exon, intron, or an intergenic region. Additionally, overlap of DMCpGs between samples and developmental stages were identified.

To identify the genes associated with the DMCpGs, bases were annotated using a custom R script. A gene was considered methylated if it was methylated in over half of the samples and had a median methylation value of >1. Genes were then filtered to have at least 5 CpGs represented, and percent methylation was calculated for each gene. Gene-specific CpGs (GS-

CpGs) were additionally identified. Lastly, gene ontology was used to test for similarities among genes with a CpG represented and was done using the GO_MWU package, which is a rank-based gene enrichment method (Wright et al., 2015). Analysis was run to test for genes enriched in biological processes, molecular function, and cellular components. A list of gene ontology terms with corresponding genes were downloaded from the Echinobase website (Arshinoff et al., 2022).

Results

Methylation patterns change during early development

To identify changes in DNA methylation patterns throughout important early developmental stages, the bismark pipeline was used to extrapolate methylation call data. Across the initial 27 samples analyzed, there was an average of 104,853,592.3 (+/- 47,235,000.29 s.d) reads per sample (Supplemental Table 2.2). When assessing the conversion efficiency of the 27 samples, the three oocyte samples (eg6, eg7, and eg8) had an average conversion efficiency of 57.13%, while the remaining 24 samples had an average conversion efficiency of 99.4% (SD 1.0%) (Supplemental Table 2.3). As a result of the low conversion efficiency, the oocyte samples were removed from subsequent analysis and moved forward with the remaining 24 samples (Figure 2.2). The remaining 24 samples had an average of 112,363,939.8 (+/- 44,046,981.13 s.d) reads per sample (Supplemental Table 2.2). Of those reads, 62.8% of the reads uniquely aligned, while 15.9% of the reads ambiguously aligned (Supplemental Table 2.2). Duplicate reads were removed, resulting in an average of 58,321,968.13 (+/- 27,269,959.52 s.d.) reads per sample. Bismark analysis breaks methylation calls into three methylation types – CpG methylation, CHG methylation, and CHH methylation. Of the average 273,006,647.3 (+/- 133,953,205.9 s.d.) CpGs

per sample, an average of 22.8% (+/- 2.8%) were methylated. Of the average 312,465,199.2 (+/- 154,491,611.5 s.d.) CHGs per sample, an average of 1.63% (+/- 1.9%) were methylated. Lastly, of the average 1,431,665,338 (+/- 717,531,582.9 s.d.) CHHs per sample, an average of 1.7% (+/- 1.9%) were methylated (Supplemental Table 2.2). To identify how methylation varies throughout early developmental stages, percent methylation for CpG methylation, CHG methylation, and CHH methylation were quantified for each of the eight developmental stages for each of the three genotypes, and values from the three genotypes were averaged together to generate one value per developmental stage for each methylation type (Figure 2.2). Methylation during early development was not consistent for all developmental stages. For the three methylation types, the percent methylation followed similar variation throughout early developmental stages, increasing until the blastula stage where it peaked to 26.8% CpG methylation, then decreasing during the prism and pluteus stage where it plateaued to 20.2% CpG methylation (Figure 2.2; Supplemental Table 2.2).

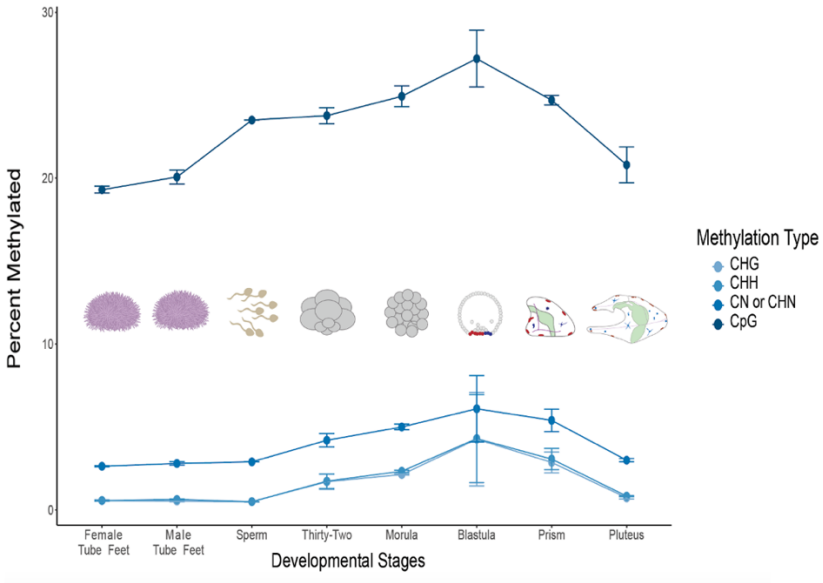

Figure 2.2: Genome percent methylation in somatic cells, sperm, and five early developmental timepoints. Points represent the mean percent methylation for each cell type

across the three genotypes. Standard error is reported as error bars. Methylation types are denoted in various shades of blue.

Methylation sites significantly vary by both developmental stage and genotype

After filtering and merging the methylation calls for the eight developmental stages across the three genotypes, 63,856 CpG sites were shared across the 24 samples. This data was used for the subsequent analyses. A principal correlation analysis (PcoA) using a Manhattan distance was used to identify the proportion of variance between developmental stages and genetic cross in their methylation profiles. Significant variation in methylation profiles between the eight developmental stages were identified (PERMANOVA; p=0.002; Figure 2.3B) as well as a significant variation in methylation profiles between the three genetic crosses (PERMANOVA; p=0.001; Figure 2.3B). The *ordiellipse* function from the *vegan* package was used to visualize standard error between the three genetic crosses and *ordispider* to connect the corresponding developmental stages from the three genetic crosses. Pco1 explains 21.17% of the variation, while Pco2 explains 14.46% of the variation across samples (Figure 2.3B).

A dendrogram was generated using the □*ethylKit* built-in *clusterSamples* function using the ward.D method. The dendrogram identifies similar methylation profiles across the 24 samples tested, and shows that methylation profiles are similarly clustered based on genotype (Figure 2.3A). Additionally, within these clusters, male tissue types (male tube feet and sperm) for each of the three genotypes present very similar methylation profiles (Figure 2.3A).

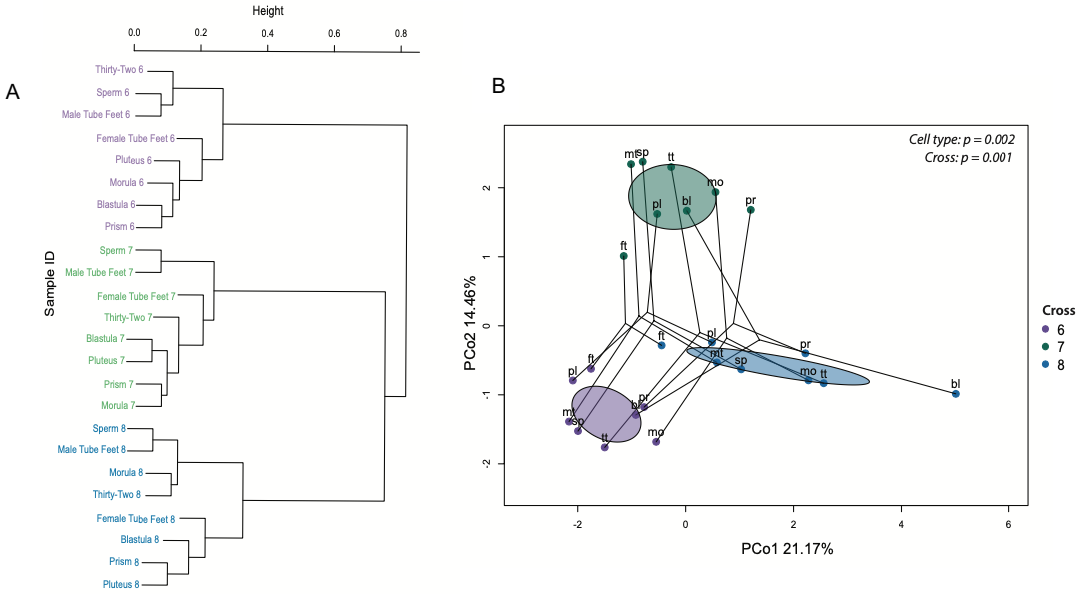

Figure 2.3: Clustering of methylation profiles of the three genotypes and the eight developmental stages. **(A)** A dendrogram and **(B)** PcoA representing the clustering of methylation profiles. Purple represents samples from cross 6, green represents samples from cross 7, and blue represents samples from cross 8.

Similarity, percent methylation between the 24 samples was visualized using a heatmap. This shows that percent methylation profiles are clustered more similarly based on genotype rather than developmental stage, with some noticeable exceptions (Figure 2.4). Similar percent methylation profiles between male tube feet, sperm, and the thirty-two cell stage were also identified, indicating that male tissue has a strong influence over the early methylation patterns of developing embryos (Figure 4). Additionally, female tube feet methylation profiles across the three genotypes were similarly clustered together, indicating a strong correlation (Figure 2.4).

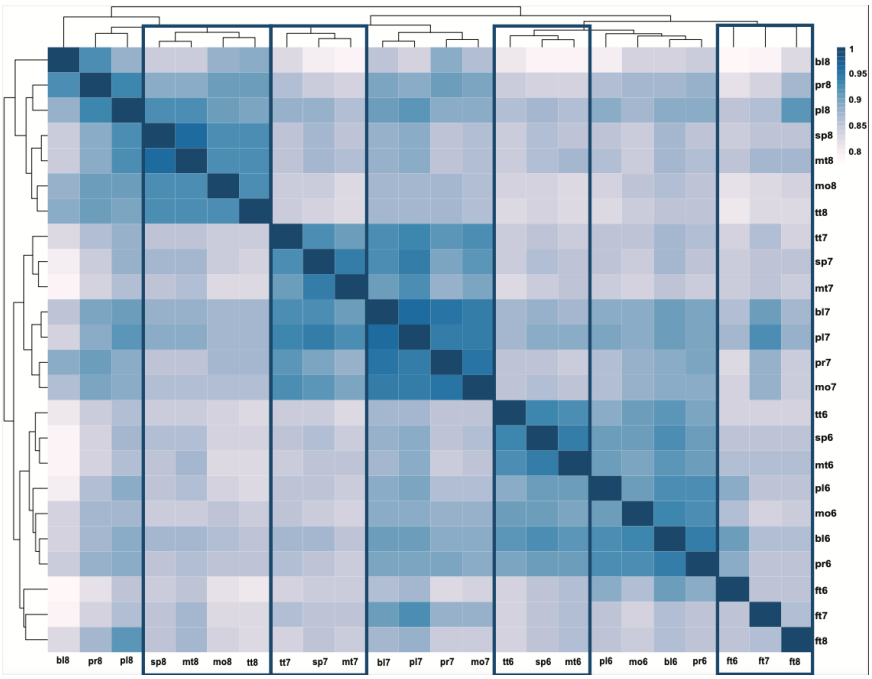

Figure 2.4: Heatmap denoting percent methylation among the 24 samples. Blue boxes denote regions of clustering of note. Abbreviations are as followed: sp=Sperm, mt=Male Tube Feet, ft=Female Tube Feet, tt= Thirty-Two Cell, mo=Morula, bl=Blastula, pr=Prism, pl=Pluteus

DMCpGs are primarily found in the intergenic region of the genome

DMCpGs were quantified for each cross and developmental stage, and identified if these DMCpG sites are hypermethylated or hypomethylated. Of the 63,856 CpG sites shared across the samples, 1046 DMCpGs are unique to Cross 6, with 478 being hypermethylated, while 568 were hypomethylated. Cross 7 contained 771 unique DMCpGs, with 382 being hypermethylated, while 389 were hypomethylated. Lastly, cross 8 contained 932 unique DMCpGs, with 567 being hypermethylated while 365 were hypomethylated (Supplemental Table 2.4). Additionally, DMCpGs were quantified for each of the eight developmental stages (Supplemental Table 2.4). Female tube feet had the highest number of unique DMCpGs among the eight developmental stages with 653 DMCpGs, 58 which were hypermethylated, while 568 were hypomethylated. The thirty-two cell stage had the least amount of DMCpGs, with only 14 unique DMCpGs, with

13 hypermethylated, and one hypomethylated (Supplemental Table 2.4). The six remaining developmental stage DMCpGs are reported in Table S.4.

Interestingly, there is very little overlap in DMCpGs across the eight sample types. The greatest overlap in shared DMCpGs occurred between male tube feet, female tube feet and sperm, with 86 shared DMCpGs (Supplemental Figure 2.4). Additionally, the sperm samples had the greatest amount of shared DMCpG sites across the other developmental stages (

Supplemental Figure **2.1**). Overlap of DMCpG sites between male tube feet and the developmental stages, as well as the female tube feet and the development stages show some overlap in shared DMCpGs between the respective tube feet and the blastula stage (Supplemental Figure 2.2, Supplemental Figure 2.3). Overlap of DMCpGs between the three genetic crosses were identified and found that there were only six DMCpG sites that were shared across all three genotypes (Supplemental Figure 2.5).

After identifying the DMCpGs between the developmental stages and the genetic crosses, we sought to identify where in the genomic region these DMCpGs are occurring. Majority of the DMCpGs occur primarily in intergenic regions and in introns, with DMCpGs having a low occurrence rate in exon and promotor regions in the genomic region (Figure 2.5). A full list of annotated DMCpGs with counts can be found in Supplemental Table 2.5.

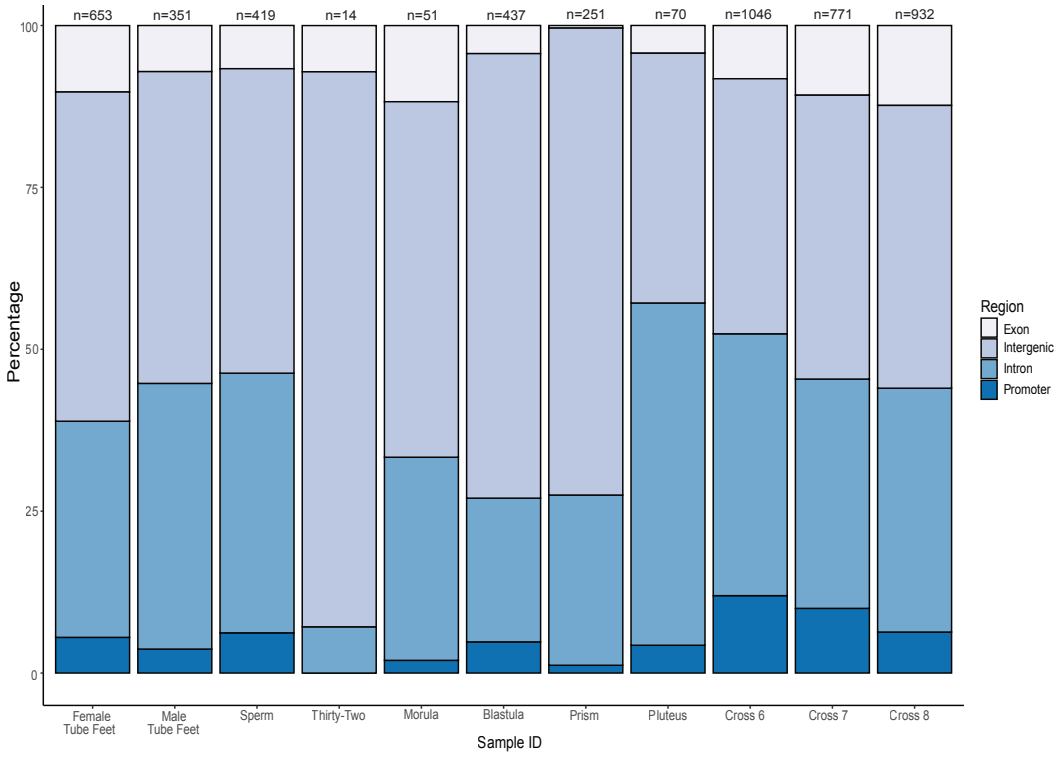

Figure 2.5*:* Location of DMCpGs in the genome. Stacked bar plots represent the location in the genomic region of the significantly different DMCpGs for both developmental stage and genetic cross (denoted as "Cross"). Regions identified are exon (light purple), intergenic (lavender), intron (light blue), and promoter (dark blue).

Identification of gene-specific DMCpGs across developmental timepoints

We sought to investigate the genes associated with the DMCpGs, and if there is variation in these genes throughout the early developmental stages. A total of 525,332 CpG sites were identified as located in gene regions shared across 1713 genes, which will be characterized as gene-specific CpGs (GS-CpGs). For GS-CpGs, a site methylated was considered methylated if it was methylated in over half of the samples (median >1), and 33,119 methylated GS-CpG sites that matched these criteria. Genes were then filtered to where there were at least 5 CpG sites per gene, and were left with 943 genes that match these criteria (Figure 2.6). This resulting gene

filtering shows a bimodal pattern, with genes predominantly being 100% methylated (Figure 2.6).

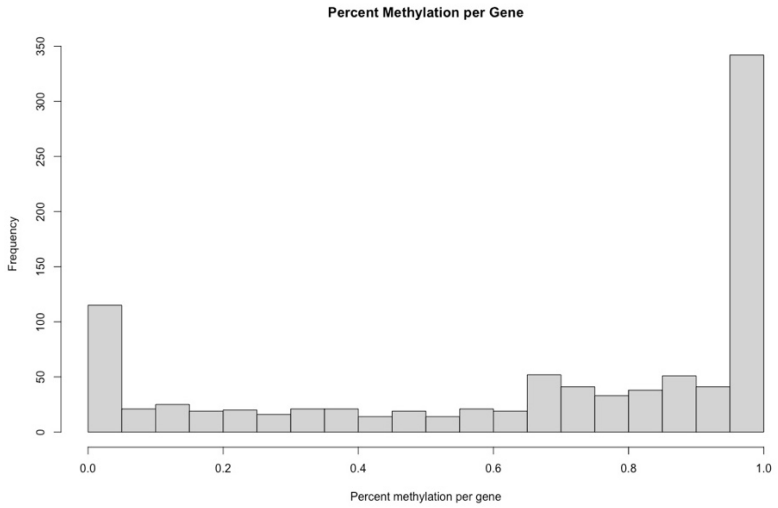

Figure 2.6: Percent methylation per gene for the 943 genes that contain at least 5 CpG sites per gene. A bimodal pattern is observed, with genes either being fully methylated or unmethylated.

We next identified if there is overlap between the DMCpGs and GS-CpGS. Overall, for the combined developmental stages, 1304 unique DMCpGs which are GS-CpGs across 287 genes were identified. Specifically, female tube feet contained 580 DMCpGs that are also GS-CpGs across 141 unique genes while male tube feet contained 307 DMCpGs which are GS-CpGs across 73 unique genes. These genes are primarily associated with protein coupled receptors, and various enzymatic functions (Supplemental Table 2.6). Sperm contained the most DMCpGs that are also GS-CpGS with 375 sites across 121 unique genes, with genes associated with various protein functions. Interestingly, male and female tube feet and sperm cells were the only developmental stages that had a DMCpG located within a methyltransferase gene.

The thirty-two stage had the least amount of DMCpGs that are also GS-CpGs, with only 11 sites found across seven unique genes, with majority of the sites occurring in the gene which

codes for amidotransferases. The morula stage contained 46 DMCpGs that are also GS-CpGs across 25 unique genes, with an increase in sites occurring in the gene which catalyzes transcription, while the blastula stage contained 335 DMCpGs that are also GS-CpGs across 110 unique genes, including ones that control sorting protein and aminotransferases. There is a decrease in the prism stage, with 198 DMCpGs that are also GS-CpGs across 82 unique genes, while the pluteus stage contained only 69 DMCpGs that are also GS-CpGs across 34 unique genes (Supplemental Table 2.6). Across the three different genotypes sampled, a total of 1739 DMCpGs that are also GS-CpGs across 252 genes were found. Specifically, cross 6 contained 868 DMCpGs that are also GS-CpGs across 137 genes, with genes associated with RNA polymerases, and protein ligases highly represented. Cross 7 contained 587 DMCpGs that are also GS-CpGs across 140 genes. Lastly, cross 8 contained 768 DMCpGs that are also GS-CpGs across 138 genes, with genes associated with methyltransferases, protein functions, and phosphate transporters highly represented (Supplemental Table 2.6).

Using the GO_MWU package, no significantly enriched genes associated with cellular components or biological processes were found across the genotypes and the developmental stages sampled. However, significantly enriched genes among genes involved in molecular functions were identified. Genes associated with protein dimerization activity (GO:0046983) were significantly enriched in cross 7 and cross 8, as well as sperm, thirty-two cell, prism, and male and female tube feet. Genes associated with the structural constituent of chromatin (GO:0030527) were significantly enriched in cross 7, sperm, thirty-two cell, morula, and male and female tube feet, while genes associated with protein binding (GO:0005515) were significantly enriched in female tube feet. Lastly, genes associated with DNA binding

(GO:0003677) were significantly enriched in cross 7, thirty-two cell, and male and female tube feet.

Discussion

In this study, the change in DNA methylation patterns throughout eight important developmental stages and between three distinct genetic crosses in *Strongylocentrotus pupuratus*, an ecologically important marine invertebrate was categorized. Genomic DNA methylation patterns vary significantly between the eight distinct sample types as well as between the genotypic crosses, indicating that many factors contribute to the complexity of DNA methylation patterns in *S. purpuratus*. Additionally, differentially methylated CpGs are predominately found in the intergenic regions across all samples, indicating that DNA methylation plays an important role in the regulation of gene expression during embryogenesis and early development. These data add to a growing literature base on the variation, influence, and importance of DNA methylation in organisms, specifically through embryogenesis and development.

Eight important tissue types including adult somatic cells, gametes, and early developmental stages were used to categorize DNA methylation patterns in *S. purpuratus*. Our samples fully encapsulate the three developmental periods of a sea urchin (embryonic period, planktonic period, and adult period) (Figure 2.1). Additionally, methylation information was extracted from oocytes of the three adult females used, however, we were unable to progress further with those samples due to a low conversion efficiency (average of 57.13% efficiency). Although unfortunate, the remaining samples provide a comprehensive window into variation in DNA methylation patterns during embryogenesis and the influence of genotype on these patterns. We utilized three distinct genetic crosses for our experiment in attempt to extrapolate if

and what the influence of genotype plays in methylation patterns of their offspring. Previous research has categorized the influence of genotype on DNA methylation patterns in offspring (Asselman et al., 2015; Silliman et al., 2023), and has shown that it can contribute significantly to offspring methylation profiles.

Methylation patterns changes during development

A variation in percent methylation between the eight developmental stages was identified, with percent methylation increasing after fertilization until reaching the blastula stage, where percent methylation peaked at 26.8% methylated in CpG context (Figure 2.2). After the blastula stage, the global percent methylation decreased until it reached 20.8% CpG methylated for the pluteus stage. Percent methylation profiles for the purple sea urchin have been categorized as well in (Xu et al., 2019), however our results differ slightly compared to their findings, specifically in the percent methylation of sperm. Xu et al. found that sperm was the most heavily methylated of the developmental stages analyzed, at around 27.5%, however, our results show that sperm was 23.5% methylated. Although a 4% difference, this variation is of note. Xu et al,. used whole genome bisulfite sequencing (WGBS) for methylation extraction, while we used EM-seq. WGBS has been shown to overestimate methylation levels compared to EM-seq, so this may be contributing to the variation observed in these results (Feng et al., 2020). Despite our inability to quantify percent methylation of the oocytes due to the low conversion rate, previous research has quantified percent methylation of this developmental stage and found that oocytes are approximately 23% methylated in the purple sea urchin (Xu et al., 2019). This is a notable observation, as this value closely resembles our observed sperm methylation percent. Percent methylation changes have been observed for other marine invertebrates with variation observed

across developmental timepoints. Most notably, the oyster (*C. gigas*) has a similar percent methylation profile as the purple sea urchin, where global percent methylation peaks at the blastula stage, and then decreases as development progresses (Riviere et al., 2013).

Interestingly, the global percent methylation patterns at the pluteus stage of the purple sea urchin decreases to the levels observed at the adult tube feet stage. This variation in percent methylation could be attributed to the DNA-methyltransferases (DNMT) enzymes. DNMTs are extremely conserved and highly regulated during the initial stages of sea urchin early development (Aniello et al., 1996), with DNMT activity peaking at the blastula stage, and decreasing to a constant state at the prism and pluteus stage (Aniello et al., 2003; Tosi et al., 1995). The observations here indicate that variation in percent methylation through development could potentially be explained by this DNMT activity. Future work should identify methylation patterns in later stage pluteus (6-arm stage and beyond) and metamorphosis to see if and how percent methylation in the genome changes as development progresses, or if the patters remain similar.

DNA methylation is highly influenced by genetic background

We identified a significant difference in methylation profiles between the developmental stages and across the three genetic crosses (Figure 2.3). Methylation profiles are predominantly clustered by genetic cross, suggesting that methylation patterns are inherited. Previous research has identified variation methylation profiles by genotype in the Olympia oyster (*Ostrea lurida)* and found that one third of the variation in methylation attributed to genotype (Silliman et al., 2023). The role of genetic background on the epigenetic patterning of offspring is an important consideration. Non-genetic inheritance from parent to offspring can influence the success of the

offspring. Parental conditions can result in gametically induced changes to produce adaptive phenotypes in offspring exposed to similar stresses, allowing the offspring to be more successful in this environment (Adrian-Kalchhauser et al., 2020).

We found that male developmental stages (sperm and male tube feet) have similar methylation profiles as the thirty-two cell stage across all three genetic crosses, indicating that males have a strong influence over methylation patterns of their offspring. Since we do not have oocyte samples for comparison, we must solely rely on the female tube feet samples to make conclusions on maternal influences on methylation patterns of their offspring. Even so, we cannot know for certain if males are predominately influencing methylation patterns, or if there in an interplay of both maternal and paternal factors influencing these patterns. However, previous research has categorized maternal effects on larval DNA methylation profiles of *S. purpuratus* when exposed to various environmental stressors and found that there are maternal influences driving the methylation patterns of their progeny (Strader et al., 2019, 2020). Future work will seek to identify the influence of oocytes on DNA methylation patterns on their offspring.

Methylation sites significantly vary by developmental stage

Interestingly, there was also a significant difference in DNA methylation profiles between the eight developmental stages. Similar results have been observed in the common octopus (*O. vulgaris),* where researchers found that paralarvae have a distinct methylation profile compared to mature adult samples (Díaz-Freije et al., 2014). Additionally, percent methylation of the 24-samples was visualized using a heatmap (Figure 2.4), and identified similar trends in percent methylation patterns, with clustering predominantly associated with genotype. An interesting

exception was documented, with the three female tube feet samples clustering together rather than with their respective genotypes, which was not observed in the male tube feet samples. Our results indicate an interplay of genotype and developmental stage influencing methylation patterns.

DMCpGs are primarily found in the intergenic region of the genome

We next calculated differentially methylated CpG sites across the developmental stage, and for the three genetic crosses, and found that female tube feet had the greatest amount of DMCpGs at 653 sites. For the developmental stages, the blastula stage had the most DMCpG sites at 437, while the thirty-two cell stage had the least, with only 14 DMCpGs. Additionally, we characterized the location of DMCpGs across our samples and found that they were located predominantly in the in intergenic and intron regions of the genome, with relatively few sites occurring in the promoter and exon region of the genome (Figure 2.5). This paints an interesting picture of the distribution and function of DNA methylation across the genome. Previous research has categorized that targets of DNA methylation in invertebrates are concentrated in CpGs in gene bodies and not in the promoter region (Feng et al., 2010; Keller et al., 2016; Sarda et al., 2012; Zemach et al., 2010), and we see this pattern of DMCpGs in the intron for our samples. DNA methylation of CpGs concentrated in gene bodies are associated with active transcription of genes (Keller et al., 2016) and show less expression variability compared to other gene by lowering transcriptional noise (A. Bird, 1995; Huh et al., 2013; Keller et al., 2016; Zemach et al., 2010). Additionally, in invertebrates, heavily methylated gene bodies have increased expression (Keller et al., 2016; Sarda et al., 2012; Suzuki et al., 2007). Somewhat similar methylation profiles in other marine invertebrates have been reported. For instance, in

cnidarians, DNA methylation is primarily concentrated in introns, while promoters and intergenic regions were predominantly absent of DNA methylation (Ying et al., 2022). Although we see an increase in methylation occurring in the intergenic region for our samples, this shared methylation of introns across marine invertebrates shows that this pattern is relatively universal in metazoans. Intronic methylation has been suggested to be involved in gene regulation by expressing alternate isoforms of genes (Gavery & Roberts, 2013). Additionally, when DNA methylation is concentrated in intronic regions, transcription is increased due to the recruitment of histone modifiers and chromatin remodelers (Dhar et al., 2021).

Identification of gene-specific DMCpGs across developmental timepoints

We identified gene-specific DMCpGs (GS-CpGs) across the stages and genotypes sampled and found that the genes associated with the GS-CpGs have a wide range of functions and characteristics. For instance, the gene for an adhesion G-protein coupled receptor was differentially methylated in all samples except for the pluteus stage and has been shown to be involved in cell migration and adhesion (Peeters et al., 2015). Additionally, a sizable number of GS-CpGs occurring at genes that are involved in protein ubiquitination. Protein ubiquitination is critical for protein degradation and synthesis and is also a post translational modification (Komander, 2009; Peng et al., 2003; Venkataraman et al., 2020). Previous research identifying variation in differential methylation in the eastern oyster (*Crassostrea virginica*) also saw majority of the differentially methylated loci identified occurred in genes associated with protein ubiquitination, specifically in reproductive tissue (Venkataraman et al., 2020). Protein ubiquitination serves many functions, including DNA repair, cell signaling, and apoptosis, and dysregulation can have major consequences for cells (Damgaard, 2021).

Functional enrichment

Gene ontology was run to identify gene enrichment for each developmental stage and for each genotype. Only GO terms for molecular function were significantly enriched, with no significant enrichment in biological processes or cellular components identified. For molecular function, particularly in the female tube feet samples, genes were significantly enriched code for DNA binding, protein binding, protein dimerization, and structural constituent of chromatin, which all play an important role in DNA methylation and gene expression. Protein dimerization is an important subset of protein-protein interactions, and can result in a larger interactive surface, which can lead to increased DNA-protein or protein-protein interactions (Klemm et al., 1998). Also, dimerization between DNA binding proteins plays an important role cooperative DNA binding (Klemm et al., 1998). Methylated cytosines can contribute to protein binding, as methylated cytosines can act as binding platforms for specific proteins or prevent protein binding to DNA (Quina et al., 2006). The structural constituent of chromatin is a molecule that contributes to the structural integrity of chromatin (Dutta et al., 2017). Chromatin is critical for the regulation of gene expression as it regulates gene accessibility and replication and is an important component for DNA methylation (Quina et al., 2006). The combination of chromatin modelling activities and methyl DNA binding proteins within the same protein complex leads to a connection between chromatin alterations and DNA methylation during transcriptional repression (Quina et al., 2006). This enrichment between protein binding, and chromatin, as well as DNA binding show an interaction between the three functions which could be contributing to DNA methylation.

Overall, we identify how DNA methylation patterns vary through various stages of *Strongylocentrotus purpuratus* development, and whether genetic background influences these methylation patterns, or if they are stage specific. We find both significant differences between DNA methylation patterns between developmental stage and genotype, indicating an interactive relationship between the two. Additionally, we identify differentially methylated CpG sites (DMCpG), with most sites occurring in the intergenic region of the genome. Gene-specific DMCpGs were established, with genes associated with molecular functions significantly enriched. These results provide novel insights into the variation in DNA methylation profiles between genotypes and developmental stages of an important marine invertebrate.

Supplementary Materials

Supplemental Table 2.1: Folder containing all bismark output files. These files can be found at: https://github.com/emw0083/thesis_documents.

Supplemental Table 2.2: Spreadsheet containing alignment reads and methylation information for all the samples. This spreadsheet is included as a separate excel file and can be found at: https://github.com/emw0083/thesis_documents.

Supplemental Table 2.3: Spreadsheet containing the conversion efficiency for all samples. This spreadsheet is included as a separate excel file and can be found at: https://github.com/emw0083/thesis_documents.

Supplemental Table 2.4: Spreadsheet containing DMCpG counts for each sample, including hypermethylated and hypomethylated counts. This spreadsheet is included as a separate excel file and can be found at: https://github.com/emw0083/thesis_documents.

Supplemental Table 2.5: Spreadsheet DMCpG annotations and counts for each sample. This spreadsheet is included as a separate excel file and can be found at: https://github.com/emw0083/thesis_documents.

Supplemental Table 2.6: Gene names of GS-CpGs where five or more genes are represented.

Developmental Stage	**Gene Name**	**Count**
Sperm	uncharacterized LOC585483	5
	adhesion G-protein coupled receptor G2-like	5
	uncharacterized LOC105441402	7
	39S ribosomal protein L40, mitochondrial	7
	uncharacterized LOC105438763	6
	phosphatidylinositol N-acetylglucosaminyltransferase subunit Q	7
	sorting nexin 8	5
	uncharacterized LOC100890393	5

	glycosyltransferase 8 domain-containing protein 1	5
	cationic trypsin-like	5
	uncharacterized LOC105436494	13
	probable E3 ubiquitin-protein ligase HERC4	9
	DNA-directed RNA polymerase I subunit RPA1-like	19
	dimethylarginine dimethylaminohydrolase 1	6
	coiled-coil domain-containing protein 34-like	24
	uncharacterized LOC100889410	43
	methyltransferase like 15	7
	furin	7
Male Tube Feet	adhesion G-protein coupled receptor G2-like	16
	uncharacterized LOC105438763	7
	phosphatidylinositol N-acetylglucosaminyltransferase subunit Q	5
	sorting nexin 8	6
	prominin 1	5
	glycosyltransferase 8 domain-containing protein 1	5
	elongator complex protein 4	6
	uncharacterized LOC105436495	9
	uncharacterized LOC105436494	82
	probable E3 ubiquitin-protein ligase HERC4	6

	glutamyl-tRNA(Gln) amidotransferase subunit A, mitochondrial-like	13
	DNA-directed RNA polymerase I subunit RPA1-like	9
	uncharacterized LOC100889410	15
	uncharacterized LOC115919768	5
Female Tube Feet	ubiquitin carboxyl-terminal hydrolase 48-like	8
	uncharacterized protein K02A2.6-like	15
	uncharacterized LOC594282	6
	adhesion G-protein coupled receptor G2-like	17
	vacuolar segregation protein PEP7	12
	early histone H1	10
	sorting nexin 8	12
	uncharacterized LOC115918670	7
	G protein-coupled receptor 22	5
	probable inactive 1-aminocyclopropane-1-carboxylate synthase-like protein 2	7
	elongator complex protein 4	6
	uncharacterized LOC105436495	6
	uncharacterized LOC105436494	60
	rho GTPase-activating protein 21	7
	kinesin heavy chain	12
	probable E3 ubiquitin-protein ligase HERC4	7

	uncharacterized LOC100892411	5
	ribosomal protein L15	6
	GTPase HRas	6
	glutamyl-tRNA(Gln) amidotransferase subunit A, mitochondrial-like	16
	DNA-directed RNA polymerase I subunit RPA1-like	21
	dimethylarginine dimethylaminohydrolase 1	5
	coiled-coil domain-containing protein 34-like	46
	uncharacterized LOC100889410	36
	uncharacterized LOC115919768	5
	methyltransferase like 15	11
	alpha-1,3-mannosyl-glycoprotein 4-beta-N-acetylglucosaminyltransferase B-like	9
	UTP15 small subunit processome component	5
Thirty-Two Cell	glutamyl-tRNA(Gln) amidotransferase subunit A, mitochondrial-like	5
Morula	DNA-directed RNA polymerase I subunit RPA1-like	5
Blastula	adhesion G-protein coupled receptor G2-like	6
	uncharacterized LOC585963	5
	uncharacterized LOC105441402	10
	uncharacterized LOC105438763	8

	MIT domain-containing protein 1	5
	histone H3, embryonic	10
	sorting nexin 8	13
	lactadherin-like	5
	glycosyltransferase 8 domain-containing protein 1	5
	uncharacterized LOC105436494	17
	uncharacterized LOC115925356	5
	probable E3 ubiquitin-protein ligase HERC4	6
	glutamyl-tRNA(Gln) amidotransferase subunit A, mitochondrial-like	17
	DNA-directed RNA polymerase I subunit RPA1-like	11
	dimethylarginine dimethylaminohydrolase 1	6
	uncharacterized LOC100892542	6
	kinesin-like protein KIF13A	6
	uncharacterized LOC100889410	14
	uncharacterized LOC115919768	10
	WD repeat domain 97	6
	furin	7
	heterogeneous nuclear ribonucleoprotein K	5
Prism	uncharacterized LOC105438763	6
	uncharacterized LOC115922920	5
	intraflagellar transport 52	5

	glycosyltransferase 8 domain-containing protein 1	5
	uncharacterized LOC105436494	12
	DNA-directed RNA polymerase I subunit RPA1-like	16
	dimethylarginine dimethylaminohydrolase 1	6
	uncharacterized LOC100892542	6
	uncharacterized LOC100889410	12
	alpha-1,3-mannosyl-glycoprotein 4-beta-N-acetylglucosaminyltransferase B-like	5
Pluteus	sorting nexin 8	10
	G protein-coupled receptor 22	5
	probable E3 ubiquitin-protein ligase HERC4	6
	dehydrogenase/reductase SDR family member 11	5

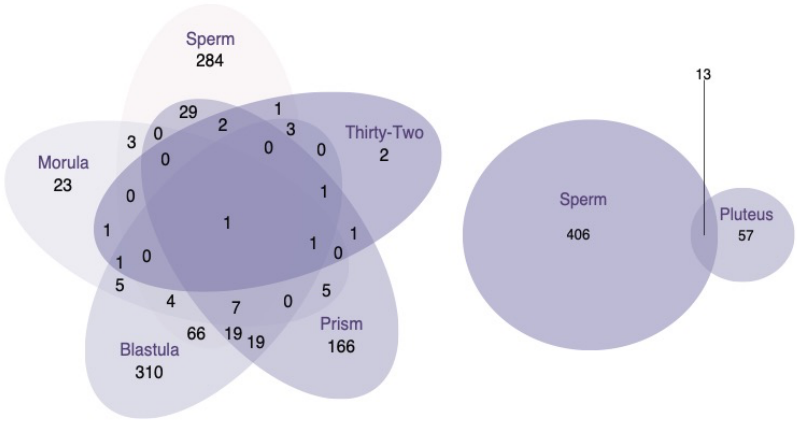

Supplemental Figure 2.1:Comparing DMCpGs across cell types occurring during embryogenesis and sperm.

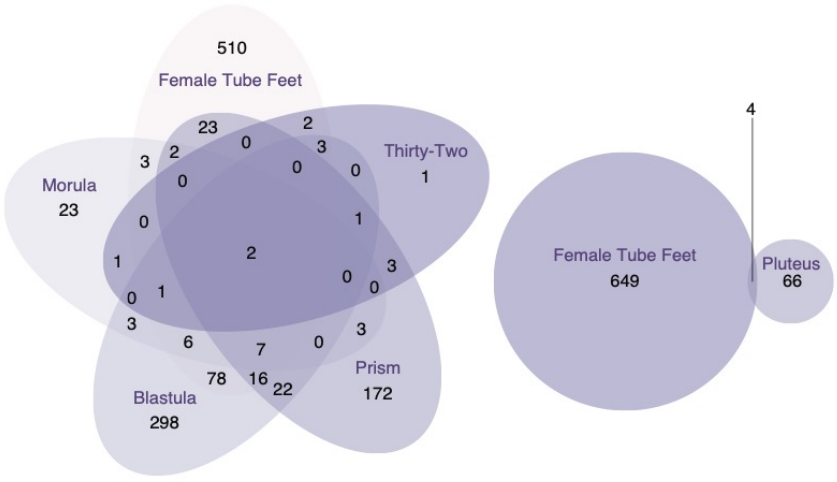

Supplemental Figure 2.2: Comparing DMCpGs across embryogenesis cell types and adult female tube feet.

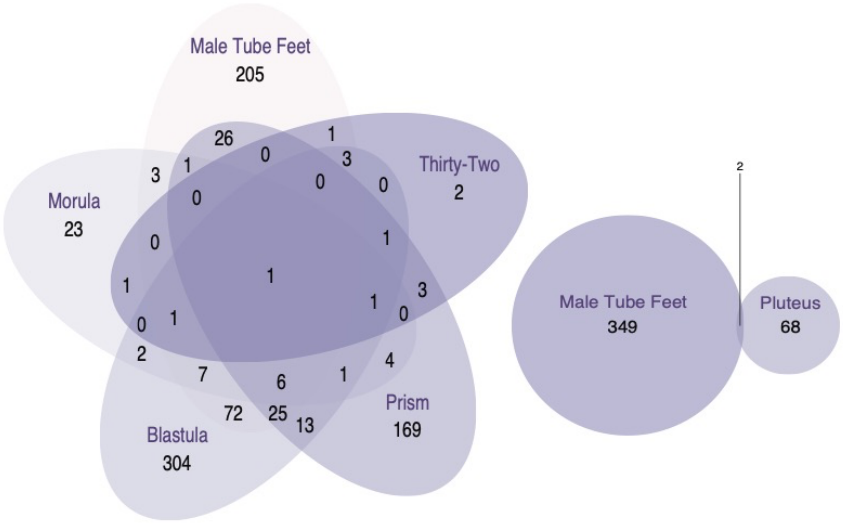

Supplemental Figure 2.3: Comparing DMCpGs across embryogenesis cell types and adult male tube feet.

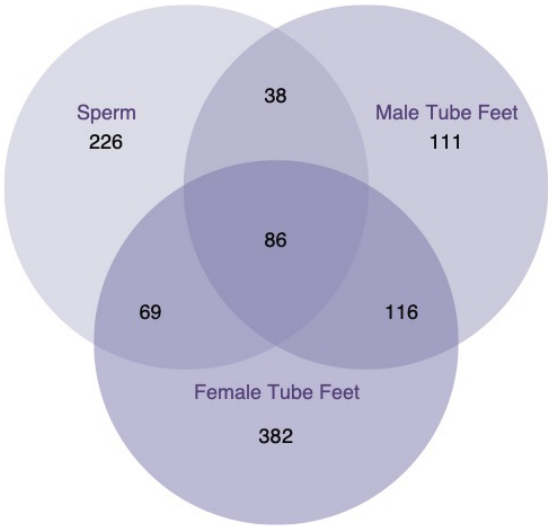

Supplemental Figure 2.4: Comparing DMCpGs between adult tube feet and sperm cells.

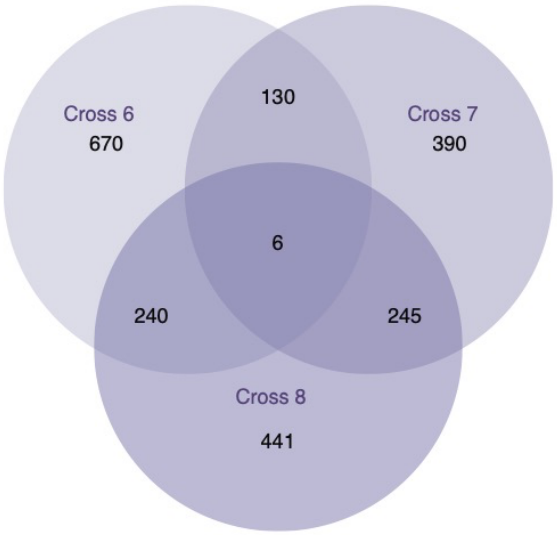

Supplemental Figure 2.5: DMCpGs similarities between the three genotypes.

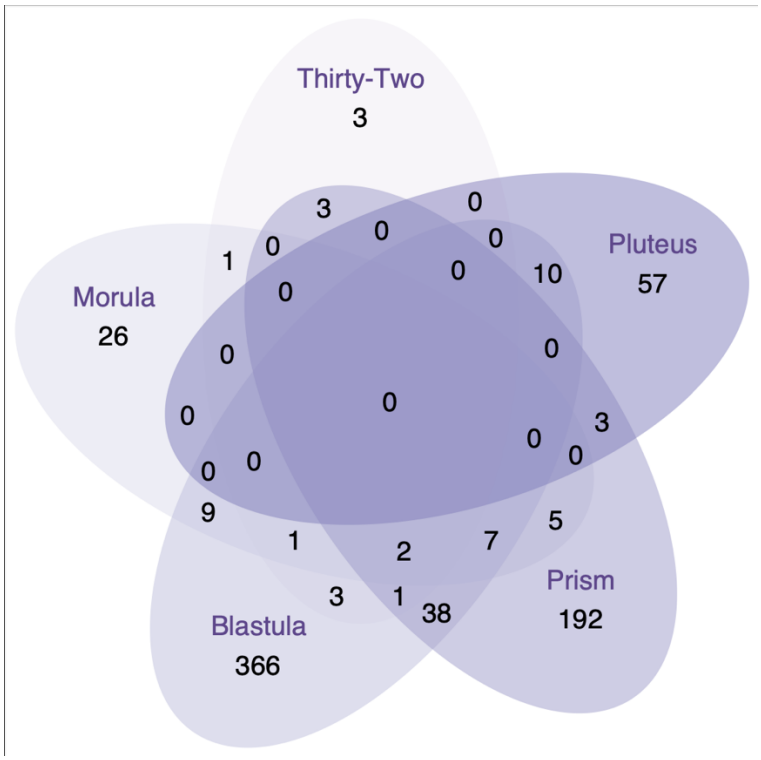

Supplemental Figure 2.6: Comparing DMCpGs across embryogenesis stages.

References

Adonin, L., Drozdov, A., & Barlev, N. A. (2021). Sea Urchin as a Universal Model for Studies of Gene Networks. In *Frontiers in Genetics* (Vol. 11). Frontiers Media S.A. https://doi.org/10.3389/fgene.2020.627259

Adrian-Kalchhauser, I., Sultan, S. E., Shama, L. N. S., Spence-Jones, H., Tiso, S., Keller Valsecchi, C. I., & Weissing, F. J. (2020). Understanding "Non-genetic" Inheritance: Insights from Molecular-Evolutionary Crosstalk. In *Trends in Ecology and Evolution* (Vol. 35, Issue 12, pp. 1078–1089). Elsevier Ltd. https://doi.org/10.1016/j.tree.2020.08.011

Akalin, A., Kormaksson, M., Li, S., Garrett-Bakelman, F. E., Figueroa, M. E., Melnick, A., & Mason, C. E. (2012). MethylKit: a comprehensive R package for the analysis of genome-wide DNA methylation profiles. *Genome Biology*, *13*(10). https://doi.org/10.1186/gb-2012-13-10-R87

Allen, J. D., & Pernet, B. (2007). Intermediate modes of larval development: Bridging the gap between planktotrophy and lecithotrophy. In *Evolution and Development* (Vol. 9, Issue 6, pp. 643–653). https://doi.org/10.1111/j.1525-142X.2007.00202.x

Alvarado, J. J., & Cortés, J. (2009). Echinoderms. In J. Wehrtmann Ingo S. and Cortés (Ed.), *Marine Biodiversity of Costa Rica, Central America* (pp. 421–433). Springer Netherlands. https://doi.org/10.1007/978-1-4020-8278-8_39

Amaya, D. J., Miller, A. J., Xie, S. P., & Kosaka, Y. (2020). Physical drivers of the summer 2019 North Pacific marine heatwave. *Nature Communications*, *11*(1). https://doi.org/10.1038/s41467-020-15820-w

Anaya, J.-M., Shoenfeld, Y., Rojas-Villarraga, A., Levy, R. A., & Cervera, R. (2013). *Autoimmunity: From Bench to Bedside*.

Aniello, F., Locascio, A., Fucci, L., Geraci, G., & Branno, M. (1996). Isolation of cDNA clones encoding DNA methyltransferase of sea urchin P. lividus: expression during embryonic development. In *GENE AN INTERNATIONAL JOURNAl,-ON GENES AND GENOHES* (Vol. 178).

Aniello, F., Villano, G., Corrado, M., Locascio, A., Russo, M. T., D'aniello, S., Francone, M., Fucci, L., & Branno, M. (2003). *Structural organization of the sea urchin DNA (cytosine-5)-methyltransferase gene and characterization of five alternative spliced transcripts*. www.elsevier.com/locate/gene

Arnone, M. I., Byrne, M., & Martinez, P. (2015). Echinodermata. In A. Wanninger (Ed.), *Evolutionary Developmental Biology of Invertebrates 6: Deuterostomia* (pp. 1–58). Springer Vienna. https://doi.org/10.1007/978-3-7091-1856-6_1

Arshinoff, B. I., Cary, G. A., Karimi, K., Foley, S., Agalakov, S., Delgado, F., Lotay, V. S., Ku, C. J., Pells, T. J., Beatman, T. R., Kim, E., Andrew Cameron, R., Vize, P. D., Telmer, C. A., Croce, J. C., Ettensohn, C. A., & Hinman, V. F. (2022). Echinobase: Leveraging an extant model organism database to build a knowledgebase supporting research on the genomics and biology of echinoderms. *Nucleic Acids Research*, *50*(D1), D970–D979. https://doi.org/10.1093/nar/gkab1005

Asselman, J., De Coninck, D. I. M., Vandegehuchte, M. B., Jansen, M., Decaestecker, E., De Meester, L., Vanden Bussche, J., Vanhaecke, L., Janssen, C. R., & De Schamphelaere, K. A. C. (2015). Global cytosine methylation in Daphnia magna depends on genotype,

environment, and their interaction. *Environmental Toxicology and Chemistry*, *34*(5), 1056–1061. https://doi.org/10.1002/etc.2887

Bannister, A. J., & Kouzarides, T. (2011). Regulation of chromatin by histone modifications. In *Cell Research* (Vol. 21, Issue 3, pp. 381–395). https://doi.org/10.1038/cr.2011.22

Barela Hudgell, M. A., Grayfer, L., & Smith, L. C. (2022). Coelomocyte populations in the sea urchin, Strongylocentrotus purpuratus, undergo dynamic changes in response to immune challenge. *Frontiers in Immunology*, *13*. https://doi.org/10.3389/fimmu.2022.940852

Bates, D., Mächler, M., Bolker, B. M., & Walker, S. C. (2015). Fitting linear mixed-effects models using lme4. *Journal of Statistical Software*, *67*(1). https://doi.org/10.18637/jss.v067.i01

Beal, A., Rodriguez-Casariego, J., Rivera-Casas, C., Suarez-Ulloa, V., & Eirin-Lopez, J. M. (2020). Environmental Epigenomics and Its Applications in Marine Organisms. In O. P. Oleksiak Marjorie F. and Rajora (Ed.), *Population Genomics: Marine Organisms* (pp. 325–359). Springer International Publishing. https://doi.org/10.1007/13836_2018_28

Beaugrand, G., Edwards, M., Brander, K., Luczak, C., & Ibanez, F. (2008). Causes and projections of abrupt climate-driven ecosystem shifts in the North Atlantic. *Ecology Letters*, *11*(11), 1157–1168. https://doi.org/10.1111/j.1461-0248.2008.01218.x

Bird, A. (1995). *Gene number, noise reduction and biological complexity*.

Bird, A. (2002). DNA methylation patterns and epigenetic memory. In *Genes and Development* (Vol. 16, Issue 1, pp. 6–21). https://doi.org/10.1101/gad.947102

Bird, A. P., & Taggart, M. H. (1980). Variable patterns of total DNA and rDNA methylation in animals. In *Nucleic Acids Research* (Vol. 8).

Bogan, S. N., Strader, M. E., & Hofmann, G. E. (2023). Associations between DNA methylation and gene regulation depend on chromatin accessibility during transgenerational plasticity. *BMC Biology*, *21*(1). https://doi.org/10.1186/s12915-023-01645-8

Bosch, I., Beauchamp, K. A., Steele, M. E., & Pearse, J. S. (1987). *DEVELOPMENT, METAMORPHOSIS, AND SEASONAL ABUNDANCE OF EMBRYOS AND LARVAE OF THE ANTARCTIC SEA URCHIN STERECHINUS NEUMA YERI*.

Bossdorf, O., Richards, C. L., & Pigliucci, M. (2008). Epigenetics for ecologists. In *Ecology Letters* (Vol. 11, Issue 2, pp. 106–115). https://doi.org/10.1111/j.1461-0248.2007.01130.x

Branco, P. C., Pressinotti, L. N., Borges, J. C. S., Iunes, R. S., Kfoury, R., da Silva, M. O., Gonzalez, M., dos Santos, M. F., Peck, L. S., Cooper, E. L., & da Silva, R. M. C. (2012). Cellular biomarkers to elucidate global warming effects on Antarctic sea urchin Sterechinus neumayeri. *Polar Biology*, *35*(2), 221–229. https://doi.org/10.1007/s00300-011-1063-5

Brierley, A. S., & Kingsford, M. J. (2009). Impacts of Climate Change on Marine Organisms and Ecosystems. In *Current Biology* (Vol. 19, Issue 14). https://doi.org/10.1016/j.cub.2009.05.046

Buckley, K. M., & Rast, J. P. (2019). Immune activity at the gut epithelium in the larval sea urchin. In *Cell and Tissue Research* (Vol. 377, Issue 3, pp. 469–474). Springer Verlag. https://doi.org/10.1007/s00441-019-03095-7

Burge, C. A., Mark Eakin, C., Friedman, C. S., Froelich, B., Hershberger, P. K., Hofmann, E. E., Petes, L. E., Prager, K. C., Weil, E., Willis, B. L., Ford, S. E., & Harvell, C. D. (2014). Climate change influences on marine infectious diseases: Implications for management and society. *Annual Review of Marine Science*, *6*, 249–277. https://doi.org/10.1146/annurev-marine-010213-135029

Byers, J. E. (2020). *Marine Parasites and Disease in the Era of Global Climate Change*. https://doi.org/10.1146/annurev-marine-031920

Calvin, K., Dasgupta, D., Krinner, G., Mukherji, A., Thorne, P. W., Trisos, C., Romero, J., Aldunce, P., Barrett, K., Blanco, G., Cheung, W. W. L., Connors, S., Denton, F., Diongue-Niang, A., Dodman, D., Garschagen, M., Geden, O., Hayward, B., Jones, C., … Ha, M. (2023). *IPCC, 2023: Climate Change 2023: Synthesis Report. Contribution of Working Groups I, II and III to the Sixth Assessment Report of the Intergovernmental Panel on Climate Change [Core Writing Team, H. Lee and J. Romero (eds.)]. IPCC, Geneva, Switzerland.* (P. Arias, M. Bustamante, I. Elgizouli, G. Flato, M. Howden, C. Méndez-Vallejo, J. J. Pereira, R. Pichs-Madruga, S. K. Rose, Y. Saheb, R. Sánchez Rodríguez, D. Ürge-Vorsatz, C. Xiao, N. Yassaa, J. Romero, J. Kim, E. F. Haites, Y. Jung, R. Stavins, … C. Péan, Eds.). https://doi.org/10.59327/IPCC/AR6-9789291691647

Cavole, L. M., Demko, A. M., Diner, R. E., Giddings, A., Koester, I., Pagniello, C. M. L. S., Paulsen, M.-L., Ramirez-Valdez, A., Schwenck, S. M., Yen, N. K., Zill, M. E., & Franks, P. J. S. (2016). Biological Impacts of the 2013-2015 Warm-Water Anomaly in the Northeast Pacific: Winners, Losers, and the Future. *Oceanography*, *29*(2), 273–285. https://doi.org/10.2307/24862690

Checkley, D. M., & Barth, J. A. (2009). Patterns and processes in the California Current System. *Progress in Oceanography*, *83*(1–4), 49–64. https://doi.org/10.1016/j.pocean.2009.07.028

Christensen, H. N., Oxender, D. L., Liang, M., & Vatz, K. A. (1965). *The Use of WMethylation to Direct the Route of Mediated Transport of Amino Acids** (Vol. 240, Issue 9).

Closek, C. J., Santora, J. A., Starks, H. A., Schroeder, I. D., Andruszkiewicz, E. A., Sakuma, K. M., Bograd, S. J., Hazen, E. L., Field, J. C., & Boehm, A. B. (2019). Marine Vertebrate Biodiversity and Distribution Within the Central California Current Using Environmental DNA (eDNA) Metabarcoding and Ecosystem Surveys. *Frontiers in Marine Science*, *6*. https://doi.org/10.3389/fmars.2019.00732

Cohen, R. E., James, C. C., Lee, A., Martinelli, M. M., Muraoka, W. T., Ortega, M., Sadowski, R., Starkey, L., Szesciorka, A. R., Timko, S. E., Weiss, E. L., & Franks, P. J. S. (2018). *MARINE HOST-PATHOGEN DYNAMICS: Influences of Global Climate Change*. *31*(2), 182–193. https://doi.org/10.2307/26542664

Couch, J. A., & Fournie, J. W. (1993). *CRC Series in ADVANCES in FISHERIES SCIENCE PATHOBIOLOGY of MARINE and ESTUARINE ORGANISMS Edited*.

Dabe, E. C., Sanford, R. S., Kohn, A. B., Bobkova, Y., & Moroz, L. L. (2015). DNA Methylation in Basal Metazoans: Insights from Ctenophores. *Integrative and Comparative Biology*, *55*(6), 1096–1110. https://doi.org/10.1093/icb/icv086

Damgaard, R. B. (2021). The ubiquitin system: from cell signalling to disease biology and new therapeutic opportunities. In *Cell Death and Differentiation* (Vol. 28, Issue 2, pp. 423–426). Springer Nature. https://doi.org/10.1038/s41418-020-00703-w

Deans, C., & Maggert, K. A. (2015). What do you mean, "Epigenetic"? *Genetics*, *199*(4), 887–896. https://doi.org/10.1534/genetics.114.173492

Dellatorre, M. B., & Manahan, D. T. (2023). Increasing temperature results in higher allocation of energy to protein synthesis in sea urchin larvae (Lytechinus pictus). *Biological Bulletin*, *244*(1), 35–50. https://doi.org/10.1086/723369

Dhar, G. A., Saha, S., Mitra, P., & Nag Chaudhuri, R. (2021). DNA methylation and regulation of gene expression: Guardian of our health. In *Nucleus (India)* (Vol. 64, Issue 3, pp. 259–270). Springer. https://doi.org/10.1007/s13237-021-00367-y

Di Lorenzo, E., & Mantua, N. (2016). Multi-year persistence of the 2014/15 North Pacific marine heatwave. *Nature Climate Change*, *6*(11), 1042–1047. https://doi.org/10.1038/nclimate3082

Díaz-Freije, E., Gestal, C., Castellanos-Martínez, S., & Morán, P. (2014). The role of DNA methylation on Octopus vulgaris development and their perspectives. *Frontiers in Physiology*, *5 FEB*. https://doi.org/10.3389/fphys.2014.00062

Dixon, G., & Matz, M. (2022). Changes in gene body methylation do not correlate with changes in gene expression in Anthozoa or Hexapoda. *BMC Genomics*, *23*(1). https://doi.org/10.1186/s12864-022-08474-z

Dutta, A., Sardiu, M., Gogol, M., Gilmore, J., Zhang, D., Florens, L., Abmayr, S. M., Washburn, M. P., & Workman, J. L. (2017). Composition and Function of Mutant Swi/Snf Complexes. *Cell Reports*, *18*(9), 2124–2134. https://doi.org/10.1016/j.celrep.2017.01.058

Feng, S., Cokus, S. J., Zhang, X., Chen, P. Y., Bostick, M., Goll, M. G., Hetzel, J., Jain, J., Strauss, S. H., Halpern, M. E., Ukomadu, C., Sadler, K. C., Pradhan, S., Pellegrini, M., & Jacobsen, S. E. (2010). Conservation and divergence of methylation patterning in plants and animals. *Proceedings of the National Academy of Sciences of the United States of America*, *107*(19), 8689–8694. https://doi.org/10.1073/pnas.1002720107

Feng, S., Zhong, Z., Wang, M., & Jacobsen, S. E. (2020). Efficient and accurate determination of genome-wide DNA methylation patterns in Arabidopsis thaliana with enzymatic methyl sequencing. *Epigenetics and Chromatin*, *13*(1). https://doi.org/10.1186/s13072-020-00361-9

Filbee-Dexter, K., Wernberg, T., Grace, S. P., Thormar, J., Fredriksen, S., Narvaez, C. N., Feehan, C. J., & Norderhaug, K. M. (2020). Marine heatwaves and the collapse of marginal North Atlantic kelp forests. *Scientific Reports*, *10*(1). https://doi.org/10.1038/s41598-020-70273-x

Formery, L., Wakefield, A., Gesson, M., Toisoul, L., Lhomond, G., Gilletta, L., Lasbleiz, R., Schubert, M., & Croce, J. C. (2022). Developmental atlas of the indirect-developing sea urchin Paracentrotus lividus: From fertilization to juvenile stages. *Frontiers in Cell and Developmental Biology*, *10*. https://doi.org/10.3389/fcell.2022.966408

Foster, M. C., Byrnes, J. E. K., & Reed, D. C. (2015). Effects of five southern California macroalgal diets on consumption, growth, and gonad weight, in the purple sea urchin Strongylocentrotus purpuratus. *PeerJ*, *2015*(1). https://doi.org/10.7717/peerj.719

Frölicher, T. L., Fischer, E. M., & Gruber, N. (2018). Marine heatwaves under global warming. *Nature*, *560*(7718), 360–364. https://doi.org/10.1038/s41586-018-0383-9

Gavery, M. R., & Roberts, S. B. (2013). Predominant intragenic methylation is associated with gene expression characteristics in a bivalve mollusc. *PeerJ*, *2013*(1). https://doi.org/10.7717/peerj.215

Gentleman, R. C., Carey, V. J., Bates, D. M., Bolstad, B., Dettling, M., Dudoit, S., Ellis, B., Gautier, L., Ge, Y., Gentry, J., Hornik, K., Hothorn, T., Huber, W., Iacus, S., Irizarry, R., Leisch, F., Li, C., Maechler, M., Rossini, A. J., … Zhang, J. (2004). Open Access Bioconductor: open software development for computational biology and bioinformatics. In *Genome Biology* (Vol. 5, Issue 2). http://genomebiology.com/2004/5/10/http://genomebiology.com/2004/5/10/R80

Goldsmit, J., McKindsey, C. W., Schlegel, R. W., Stewart, D. B., Archambault, P., & Howland, K. L. (2020). What and where? Predicting invasion hotspots in the Arctic marine realm. *Global Change Biology*, *26*(9), 4752–4771. https://doi.org/10.1111/gcb.15159

Gray, E. M. (2013). Thermal acclimation in a complex life cycle: The effects of larval and adult thermal conditions on metabolic rate and heat resistance in Culex pipiens (Diptera: Culicidae). *Journal of Insect Physiology*, *59*(10), 1001–1007. https://doi.org/10.1016/j.jinsphys.2013.08.001

Groner, M. L., Maynard, J., Breyta, R., Carnegie, R. B., Dobson, A., Friedman, C. S., Froelich, B., Garren, M., Gulland, F. M. D., Heron, S. F., Noble, R. T., Revie, C. W., Shields, J. D., Vanderstichel, R., Weil, E., Wyllie-Echeverria, S., & Harvell, C. D. (2016). Managing marine disease emergencies in an era of rapid change. In *Philosophical Transactions of the Royal Society B: Biological Sciences* (Vol. 371, Issue 1689). Royal Society of London. https://doi.org/10.1098/rstb.2015.0364

Hadfield, M. G., & Strathmann, M. F. (1996). *Variability, flexibility and plasticity in life histories of marine invertebrates*.

Harris, L. G., & Eddy, S. D. (2015). Sea Urchin Ecology and Biology. In *Echinoderm Aquaculture* (pp. 1–24). Wiley Blackwell. https://doi.org/10.1002/9781119005810.ch1

Harvell, C. D., Kim, K., Burkholder, J. M., Colwell, R. R., Epstein, P. R., Grimes, D. J., Hofmann, E. E., Lipp, E. K., Osterhaus, A. D. M. E., Overstreet, R. M., Porter, J. W., Smith, G. W., & Vasta, G. R. (1999). *R E V I E W : M A R I N E E C O L O G Y Emerging Marine Diseases-Climate Links and Anthropogenic Factors*. https://www.science.org

Harvell, C. D., Montecino-Latorre, D., Caldwell, J. M., Burt, J. M., Bosley, K., Keller, A., Heron, S. F., Salomon, A. K., Lee, L., Pontier, O., Pattengill-Semmens, C., & Gaydos, J. K. (2019). *Disease epidemic and a marine heat wave are associated with the continental-scale collapse of a pivotal predator (Pycnopodia helianthoides)*. https://www.science.org

Hastings, R. A., Rutterford, L. A., Freer, J. J., Collins, R. A., Simpson, S. D., & Genner, M. J. (2020). Climate Change Drives Poleward Increases and Equatorward Declines in Marine Species. *Current Biology*, *30*(8), 1572-1577.e2. https://doi.org/10.1016/j.cub.2020.02.043

Hearn, J., Pearson, M., Blaxter, M., Wilson, P. J., & Little, T. J. (2019). Genome-wide methylation is modified by caloric restriction in Daphnia magna. *BMC Genomics*, *20*(1). https://doi.org/10.1186/s12864-019-5578-4

Hibino, T., Loza-Coll, M., Messier, C., Majeske, A. J., Cohen, A. H., Terwilliger, D. P., Buckley, K. M., Brockton, V., Nair, S. V., Berney, K., Fugmann, S. D., Anderson, M. K., Pancer, Z., Cameron, R. A., Smith, L. C., & Rast, J. P. (2006). The immune gene repertoire encoded in the purple sea urchin genome. *Developmental Biology*, *300*(1), 349–365. https://doi.org/10.1016/j.ydbio.2006.08.065

Ho, E. C. H., Buckley, K. M., Schrankel, C. S., Schuh, N. W., Hibino, T., Solek, C. M., Bae, K., Wang, G., & Rast, J. P. (2016a). Perturbation of gut bacteria induces a coordinated cellular immune response in the purple sea urchin larva. *Immunology and Cell Biology*, *94*(9), 861–874. https://doi.org/10.1038/icb.2016.51

Ho, E. C. H., Buckley, K. M., Schrankel, C. S., Schuh, N. W., Hibino, T., Solek, C. M., Bae, K., Wang, G., & Rast, J. P. (2016b). Perturbation of gut bacteria induces a coordinated cellular immune response in the purple sea urchin larva. *Immunology and Cell Biology*, *94*(9), 861–874. https://doi.org/10.1038/icb.2016.51

Hobday, A. J., Alexander, L. V., Perkins, S. E., Smale, D. A., Straub, S. C., Oliver, E. C. J., Benthuysen, J. A., Burrows, M. T., Donat, M. G., Feng, M., Holbrook, N. J., Moore, P. J., Scannell, H. A., Sen Gupta, A., & Wernberg, T. (2016). A hierarchical approach to defining marine heatwaves. *Progress in Oceanography*, *141*, 227–238. https://doi.org/10.1016/j.pocean.2015.12.014

Hoegh-Guldberg, O., Cai, R., Poloczanska, E. S., Brewer, P. G., Sundby, S., Hilmi, K., Fabry, V. J., Jung, S., Perry, I., Richardson, A. J., Brown, C. J., Schoeman, D., Signorini, S., Sydeman, W., Zhang, R., van Hooidonk, R., McKinnell, S. M., Turley, C., Omar, L., … Kissel, E. (2014). *30 The Ocean Coordinating Lead Authors: Lead Authors: Review Editors*.

Holoch, D., & Moazed, D. (2015). RNA-mediated epigenetic regulation of gene expression. In *Nature Reviews Genetics* (Vol. 16, Issue 2, pp. 71–84). Nature Publishing Group. https://doi.org/10.1038/nrg3863

Hsieh, C.-L. (1994). Dependence of Transcriptional Repression on CpG Methylation Density. *Molecular and Cellular Biology*, *14*(8), 5487–5494. https://doi.org/10.1128/mcb.14.8.5487-5494.1994

Huh, I., Zeng, J., Park, T., & Yi, S. V. (2013). *DNA methylation and transcriptional noise*. http://www.epigeneticsandchromatin.com/content/6/1/9

Ichiyanagi, T., Ichiyanagi, K., Miyake, M., & Sasaki, H. (2013). Accumulation and loss of asymmetric non-CpG methylation during male germ-cell development. *Nucleic Acids Research*, *41*(2), 738–745. https://doi.org/10.1093/nar/gks1117

Jombart, T. (2008). Adegenet: A R package for the multivariate analysis of genetic markers. *Bioinformatics*, *24*(11), 1403–1405. https://doi.org/10.1093/bioinformatics/btn129

Jones, P. A. (2012). Functions of DNA methylation: Islands, start sites, gene bodies and beyond. In *Nature Reviews Genetics* (Vol. 13, Issue 7, pp. 484–492). https://doi.org/10.1038/nrg3230

Kämpf, J., & Chapman, P. (2016). *Upwelling Systems of the World A Scientific Journey to the Most Productive Marine Ecosystems*. http://visibleearth.nasa.gov/view.php?id=4317

Keller, T. E., Han, P., & Yi, S. V. (2016). Evolutionary transition of promoter and gene body DNA methylation across invertebrate-vertebrate boundary. *Molecular Biology and Evolution*, *33*(4), 1019–1028. https://doi.org/10.1093/molbev/msv345

Kim, K., Dobson, A. P., Gulland, F., & Harvell, C. D. (2005). *Diseases and the Conservation of Marine Biodiversity*. https://www.researchgate.net/publication/236273467

Klemm, J. D., Schreiber, S. L., & Crabtree, G. R. (1998). DIMERIZATION AS A REGULATORY MECHANISM IN SIGNAL TRANSDUCTION. In *Annu. Rev. Immunol* (Vol. 16). www.annualreviews.org

Klughammer, J., Romanovskaia, D., Nemc, A., Posautz, A., Seid, C. A., Schuster, L. C., Keinath, M. C., Lugo Ramos, J. S., Kosack, L., Evankow, A., Printz, D., Kirchberger, S., Ergüner, B., Datlinger, P., Fortelny, N., Schmidl, C., Farlik, M., Skjærven, K., Bergthaler, A., … Bock, C. (2023). Comparative analysis of genome-scale, base-resolution DNA methylation profiles across 580 animal species. *Nature Communications*, *14*(1). https://doi.org/10.1038/s41467-022-34828-y

Komander, D. (2009). The emerging complexity of protein ubiquitination. In *Biochemical Society Transactions* (Vol. 37, Issue 5, pp. 937–953). https://doi.org/10.1042/BST0370937

Krueger, F., & Andrews, S. R. (2011). Bismark: A flexible aligner and methylation caller for Bisulfite-Seq applications. *Bioinformatics*, *27*(11), 1571–1572. https://doi.org/10.1093/bioinformatics/btr167

Kurtz, J. (2004). Memory in the innate and adaptive immune systems. In *Microbes and Infection* (Vol. 6, Issue 15, pp. 1410–1417). Elsevier Masson SAS. https://doi.org/10.1016/j.micinf.2004.10.002

Lafferty, K. D., Porter, J. W., & Ford, S. E. (2004). Are diseases increasing in the ocean? In *Annual Review of Ecology, Evolution, and Systematics* (Vol. 35, pp. 31–54). https://doi.org/10.1146/annurev.ecolsys.35.021103.105704

Laufkötter, C., Zscheischler, J., & Frölicher, T. L. (2020). *High-impact marine heatwaves attributable to human-induced global warming*. https://www.science.org

Leach, T. S., & Hofmann, G. E. (2023). Marine heatwave temperatures enhance larval performance but are meditated by paternal thermal history and inter-individual differences in the purple sea urchin, Strongylocentrotus purpuratus. *Frontiers in Physiology*, *14*. https://doi.org/10.3389/fphys.2023.1230590

Levitan, D. (1998). Does Bateman's principle apply to broadcast-spawning organisms? Egg traits influence in situ fertilization rates among congeneric sea urchins. *Evolution*, *52*(4), 1043–1056. https://doi.org/10.1111/j.1558-5646.1998.tb01832.x

Lyko, F. (2018). The DNA methyltransferase family: A versatile toolkit for epigenetic regulation. In *Nature Reviews Genetics* (Vol. 19, Issue 2, pp. 81–92). Nature Publishing Group. https://doi.org/10.1038/nrg.2017.80

Manier, M. K., & Palumbi, S. R. (2008). Intraspecific divergence in sperm morphology of the green sea urchin, Strongylocentrotus droebachiensis: Implications for selection in broadcast spawners. *BMC Evolutionary Biology*, *8*(1). https://doi.org/10.1186/1471-2148-8-283

Marshall, D. J., & Bolton, T. F. (2007). Sperm release strategies in marine broadcast spawners: The costs of releasing sperm quickly. *Journal of Experimental Biology*, *210*(21), 3720–3727. https://doi.org/10.1242/jeb.008417

Marshall, D. J., Bolton, T. F., & Keough, M. J. (2003). Offspring size affects the post-metamorphic performance of a colonial marine invertebrate. *Ecology*, *84*(12), 3131–3137. https://doi.org/10.1890/02-0311

Martin, M. (n.d.). *TECHNICAL NOTES*. http://www-huber.embl.de/users/an-

Matranga, V., Pinsino, A., Celi, M., Natoli, A., Bonaventura, R., Schröder, H. C., & Müller, W. E. G. (2005). *Monitoring Chemical and Physical Stress Using Sea Urchin Immune Cells*. https://doi.org/https://doi.org/10.1007/3-540-27683-1_5

Matranga, V., Toia, G., Bonaventura, R., & Mü Ller, W. E. G. (2000). Cellular and biochemical responses to environmental and experimentally induced stress in sea urchin coelomocytes. In *Cell Stress & Chaperones* (Vol. 5, Issue 2).

McCabe, R. M., Hickey, B. M., Kudela, R. M., Lefebvre, K. A., Adams, N. G., Bill, B. D., Gulland, F. M. D., Thomson, R. E., Cochlan, W. P., & Trainer, V. L. (2016). An unprecedented coastwide toxic algal bloom linked to anomalous ocean conditions. *Geophysical Research Letters*, *43*(19), 10,366-10,376. https://doi.org/10.1002/2016GL070023

McCallum, H., Harvell, D., & Dobson, A. (2003). Rates of spread of marine pathogens. *Ecology Letters*, *6*(12), 1062–1067. https://doi.org/10.1046/j.1461-0248.2003.00545.x

Mellin, C., Matthews, S., Anthony, K. R. N., Brown, S. C., Caley, M. J., Johns, K. A., Osborne, K., Puotinen, M., Thompson, A., Wolff, N. H., Fordham, D. A., & MacNeil, M. A. (2019). Spatial resilience of the Great Barrier Reef under cumulative disturbance impacts. *Global Change Biology*, *25*(7), 2431–2445. https://doi.org/10.1111/gcb.14625

Meyer, E., & Manahan, D. T. (2009). *Nutrient Uptake by Marine Invertebrates: Cloning and Functional Analysis of Amino Acid Transporter Genes in Developing Sea Urchins (Strongylocentrotus purpuratus)*.

Miner, C. M., Burnaford, J. L., Ambrose, R. F., Antrim, L., Bohlmann, H., Blanchette, C. A., Engle, J. M., Fradkin, S. C., Gaddam, R., Harley, C. D. G., Miner, B. G., Murray, S. N., Smith, J. R., Whitaker, S. G., & Raimondi, P. T. (2018). Large-scale impacts of sea star wasting disease (SSWD) on intertidal sea stars and implications for recovery. *PLoS ONE*, *13*(3). https://doi.org/10.1371/journal.pone.0192870

Minuti, J. J., Byrne, M., Campbell, H., Hemraj, D. A., & Russell, B. D. (2022). Live-fast-die-young: Carryover effects of heatwave-exposed adult urchins on the development of the next generation. *Global Change Biology*, *28*(19), 5781–5792. https://doi.org/10.1111/gcb.16339

Montgomery, E. M., Hamel, J. F., & Mercier, A. (2017). Ontogenetic shifts in swimming capacity of echinoderm propagules: a comparison of species with planktotrophic and lecithotrophic larvae. *Marine Biology*, *164*(3). https://doi.org/10.1007/s00227-017-3072-6

Moore, L. D., Le, T., & Fan, G. (2013). DNA methylation and its basic function. In *Neuropsychopharmacology* (Vol. 38, Issue 1, pp. 23–38). https://doi.org/10.1038/npp.2012.112

Mydlarz, L. D., Jones, L. E., & Harvell, C. D. (2006). Innate immunity, environmental drivers, and disease ecology of marine and freshwater invertebrates. In *Annual Review of Ecology, Evolution, and Systematics* (Vol. 37, pp. 251–288). https://doi.org/10.1146/annurev.ecolsys.37.091305.110103

Oliver, E. C. J., Donat, M. G., Burrows, M. T., Moore, P. J., Smale, D. A., Alexander, L. V., Benthuysen, J. A., Feng, M., Sen Gupta, A., Hobday, A. J., Holbrook, N. J., Perkins-Kirkpatrick, S. E., Scannell, H. A., Straub, S. C., & Wernberg, T. (2018). Longer and more frequent marine heatwaves over the past century. *Nature Communications*, *9*(1). https://doi.org/10.1038/s41467-018-03732-9

Padilla, D. K., & Savedo, M. M. (2013). A systematic review of phenotypic plasticity in marine invertebrate and plant systems. In *Advances in Marine Biology* (Vol. 65, pp. 67–94). Academic Press. https://doi.org/10.1016/B978-0-12-410498-3.00002-1

Pancer, Z., & Cooper, M. D. (2006). The evolution of adaptive immunity. In *Annual Review of Immunology* (Vol. 24, pp. 497–518). https://doi.org/10.1146/annurev.immunol.24.021605.090542

Pearse, J. S. (2006). Ecological role of purple sea urchins. In *Science* (Vol. 314, Issue 5801, pp. 940–941). https://doi.org/10.1126/science.1131888

Pechenik, J. A. (1999). On the advantages and disadvantages of larval stages in benthic marine invertebrate life cycles. In *MARINE ECOLOGY PROGRESS SERIES Mar Ecol Prog Ser* (Vol. 177).

Peeters, M. C., Fokkelman, M., Boogaard, B., Egerod, K. L., van de Water, B., IJzerman, A. P., & Schwartz, T. W. (2015). The adhesion G protein-coupled receptor G2 (ADGRG2/GPR64) constitutively activates SRE and NFκB and is involved in cell adhesion and migration. *Cellular Signalling*, *27*(12), 2579–2588. https://doi.org/10.1016/j.cellsig.2015.08.015

Peng, J., Schwartz, D., Elias, J. E., Thoreen, C. C., Cheng, D., Marsischky, G., Roelofs, J., Finley, D., & Gygi, S. P. (2003). A proteomics approach to understanding protein ubiquitination. In *NATURE BIOTECHNOLOGY VOLUME* (Vol. 21). http://www.nature.com/naturebiotechnology

Perry, A. L., Low, P. J., Ellis, J. R., & Reynolds, J. D. (2005). *Climate Change and Distribution Shifts in Marine Fishes*. https://www.science.org

Pineda, M. C., McQuaid, C. D., Turon, X., López-Legentil, S., Ordóñez, V., & Rius, M. (2012). Tough Adults, Frail Babies: An Analysis of Stress Sensitivity across Early Life-History

Stages of Widely Introduced Marine Invertebrates. *PLoS ONE*, *7*(10). https://doi.org/10.1371/journal.pone.0046672

Pitois, S. G., & Fox, C. J. (2006). Long-term changes in zooplankton biomass concentration and mean size over the Northwest European shelf inferred from Continuous Plankton Recorder data. *ICES Journal of Marine Science*, *63*(5), 785–798. https://doi.org/10.1016/j.icesjms.2006.03.009

Poloczanska, E. S., Burrows, M. T., Brown, C. J., Molinos, J. G., Halpern, B. S., Hoegh-Guldberg, O., Kappel, C. V., Moore, P. J., Richardson, A. J., Schoeman, D. S., & Sydeman, W. J. (2016). Responses of marine organisms to climate change across oceans. In *Frontiers in Marine Science* (Vol. 3, Issue MAY). Frontiers Media S. A. https://doi.org/10.3389/fmars.2016.00062

Preston, B. L., & Jones, R. N. (2006). *Climate Change Impacts on Australia and the Benefits of Early Action to Reduce Global Greenhouse Gas Emissions*.

Puisay, A., Pilon, R., Goiran, C., & Hédouin, L. (2018). Thermal resistances and acclimation potential during coral larval ontogeny in Acropora pulchra. *Marine Environmental Research*, *135*, 1–10. https://doi.org/10.1016/j.marenvres.2018.01.005

Putnam, H. M., & Gates, R. D. (2015). Preconditioning in the reef-building coral Pocillopora damicornis and the potential for trans-generational acclimatization in coral larvae under future climate change conditions. *Journal of Experimental Biology*, *218*(15), 2365–2372. https://doi.org/10.1242/jeb.123018

Quina, A. S., Buschbeck, M., & Di Croce, L. (2006). Chromatin structure and epigenetics. *Biochemical Pharmacology*, *72*(11), 1563–1569. https://doi.org/10.1016/j.bcp.2006.06.016

Raff, R. A., & Byrne, M. (2006). The active evolutionary lives of echinoderm larvae. In *Heredity* (Vol. 97, Issue 3, pp. 244–252). https://doi.org/10.1038/sj.hdy.6800866

Randall, C. J., & Van Woesik, R. (2015). Contemporary white-band disease in Caribbean corals driven by climate change. *Nature Climate Change*, *5*(4), 375–379. https://doi.org/10.1038/nclimate2530

Rast, J. P., Smith, L. C., Loza-Coll, M., Hibino, T., & Litman, G. W. (2006). Genomic insights into the immune system of the sea urchin. In *Science* (Vol. 314, Issue 5801, pp. 952–956). https://doi.org/10.1126/science.1134301

Reese, D. C., & Brodeur, R. D. (2006). Identifying and characterizing biological hotspots in the northern California Current. *Deep-Sea Research Part II: Topical Studies in Oceanography*, *53*(3–4), 291–314. https://doi.org/10.1016/j.dsr2.2006.01.014

Reid, P. C., Fischer, A. C., Lewis-Brown, E., Meredith, M. P., Sparrow, M., Andersson, A. J., Antia, A., Bates, N. R., Bathmann, U., Beaugrand, G., Brix, H., Dye, S., Edwards, M., Furevik, T., Gangstø, R., Hátún, H., Hopcroft, R. R., Kendall, M., Kasten, S., … Washington, R. (2010). Impacts of the oceans on climate change. In *Advances in Marine Biology* (Vol. 56). https://doi.org/10.1016/S0065-2881(09)56001-4

Rivetti, I., Fraschetti, S., Lionello, P., Zambianchi, E., & Boero, F. (2014). Global warming and mass mortalities of benthic invertebrates in the Mediterranean Sea. *PLoS ONE*, *9*(12). https://doi.org/10.1371/journal.pone.0115655

Riviere, G., Wu, G. C., Fellous, A., Goux, D., Sourdaine, P., & Favrel, P. (2013). DNA Methylation Is Crucial for the Early Development in the Oyster C. gigas. *Marine Biotechnology*, *15*(6), 739–753. https://doi.org/10.1007/s10126-013-9523-2

Roberts, S. B., & Gavery, M. R. (2012). Is there a relationship between DNA methylation and phenotypic plasticity in invertebrates? *Frontiers in Physiology*, *2 JAN*. https://doi.org/10.3389/fphys.2011.00116

Sarda, S., Zeng, J., Hunt, B. G., & Yi, S. V. (2012). The evolution of invertebrate gene body methylation. *Molecular Biology and Evolution*, *29*(8), 1907–1916. https://doi.org/10.1093/molbev/mss062

Scannell, H. A., Johnson, G. C., Thompson, L., Lyman, J. M., & Riser, S. C. (2020). Subsurface Evolution and Persistence of Marine Heatwaves in the Northeast Pacific. *Geophysical Research Letters*, *47*(23). https://doi.org/10.1029/2020GL090548

Shanks, A. L., Rasmuson, L. K., Valley, J. R., Jarvis, M. A., Salant, C., Sutherland, D. A., Lamont, E. I., Hainey, M. A. H., & Emlet, R. B. (2020). Marine heat waves, climate change, and failed spawning by coastal invertebrates. *Limnology and Oceanography*, *65*(3), 627–636. https://doi.org/10.1002/lno.11331

Sharples, J., Holt, J., & Dye, S. R. (2013). *Impacts of climate change on shelf sea stratification*. https://doi.org/10.14465/2013.arc08.067-070

Shima, J., & Findlay, A. (2002). Pelagic larval growth rate impacts benthic settlement and survival of a temperate reef fish. *MARINE ECOLOGY PROGRESS SERIES*, *235*, 303–309.

Silliman, K., Spencer, L. H., White, S. J., & Roberts, S. B. (2023). Epigenetic and Genetic Population Structure is Coupled in a Marine Invertebrate. *Genome Biology and Evolution*, *15*(2). https://doi.org/10.1093/gbe/evad013

Sin, E., Min, W. G., Kim, Y. B., & Kim, T. W. (2019). Respiration of the sea urchin Mesocentrotus nudus in response to large temperature fluctuations. *Marine Environmental Research*, *144*, 178–185. https://doi.org/10.1016/j.marenvres.2019.01.003

Singal, R., & Ginder, G. D. (1999). *DNA Methylation*. http://ashpublications.org/blood/article-pdf/93/12/4059/1654163/4059.pdf

Smale, D. A., Wernberg, T., Oliver, E. C. J., Thomsen, M., Harvey, B. P., Straub, S. C., Burrows, M. T., Alexander, L. V., Benthuysen, J. A., Donat, M. G., Feng, M., Hobday, A. J., Holbrook, N. J., Perkins-Kirkpatrick, S. E., Scannell, H. A., Sen Gupta, A., Payne, B. L., & Moore, P. J. (2019). Marine heatwaves threaten global biodiversity and the provision of ecosystem services. In *Nature Climate Change* (Vol. 9, Issue 4, pp. 306–312). Nature Publishing Group. https://doi.org/10.1038/s41558-019-0412-1

Smith, K. E., Burrows, M. T., Hobday, A. J., Gupta, A. Sen, Moore, P. J., Thomsen, M., Wernberg, T., & Smale, D. A. (2021). Socioeconomic impacts of marine heatwaves: Global issues and opportunities. In *Science* (Vol. 374, Issue 6566). American Association for the Advancement of Science. https://doi.org/10.1126/science.abj3593

Smith, K. E., Burrows, M. T., Hobday, A. J., King, N. G., Moore, P. J., Gupta, A. Sen, Thomsen, M. S., Wernberg, T., & Smale, D. A. (2023). *Biological Impacts of Marine Heatwaves*. https://doi.org/10.1146/annurev-marine-032122

Smith, L. C. (2010). Diversification of innate immune genes: Lessons from the purple sea urchin. In *DMM Disease Models and Mechanisms* (Vol. 3, Issues 5–6, pp. 274–279). https://doi.org/10.1242/dmm.004697

Smith, L. C., Rast, J. P., Brockton, V., Terwilliger, D. P., Nair, S. V, Buckley, K. M., & Majeske, A. J. (2006). The sea urchin immune system. In *ISJ* (Vol. 3).

Sodergren, E., Weinstock, G. M., Davidson, E. H., Cameron, R. A., Gibbs, R. A., Angerer, R. C., Angerer, L. M., Arnone, M. I., Burgess, D. R., Burke, R. D., Coffman, J. A., Dean, M., Elphick, M. R., Ettensohn, C. A., Foltz, K. R., Hamdoun, A., Hynes, R. O., Klein, W. H.,

Marzluff, W., … Wright, R. (2006). The genome of the sea urchin Strongylocentrotus purpuratus. *Science*, *314*(5801), 941–952. https://doi.org/10.1126/science.1133609

Strader, M. E., Kozal, L. C., Leach, T. S., Wong, J. M., Chamorro, J. D., Housh, M. J., & Hofmann, G. E. (2020). Examining the Role of DNA Methylation in Transcriptomic Plasticity of Early Stage Sea Urchins: Developmental and Maternal Effects in a Kelp Forest Herbivore. *Frontiers in Marine Science*, *7*. https://doi.org/10.3389/fmars.2020.00205

Strader, M. E., Wolak, M. E., Simon, O. M., & Hofmann, G. E. (2022). Genetic variation underlies plastic responses to global change drivers in the purple sea urchin, Strongylocentrotus purpuratus. *Proceedings of the Royal Society B: Biological Sciences*, *289*(1981). https://doi.org/10.1098/rspb.2022.1249

Strader, M. E., Wong, J. M., Kozal, L. C., Leach, T. S., & Hofmann, G. E. (2019). Parental environments alter DNA methylation in offspring of the purple sea urchin, Strongylocentrotus purpuratus. *Journal of Experimental Marine Biology and Ecology*, *517*, 54–64. https://doi.org/10.1016/j.jembe.2019.03.002

Strathmann, R. R. (1971). THE FEEDING BEHAVIOR OF PLANKTOTROPHIC ECHINODERM LARVAE: MECHANISMS, REGULATION, AND RATES OF SUSPENSION-FEEDING. In *mar. Biol. Ecol* (Vol. 6).

Strydom, S., Murray, K., Wilson, S., Huntley, B., Rule, M., Heithaus, M., Bessey, C., Kendrick, G. A., Burkholder, D., Fraser, M. W., & Zdunic, K. (2020). Too hot to handle: Unprecedented seagrass death driven by marine heatwave in a World Heritage Area. *Global Change Biology*, *26*(6), 3525–3538. https://doi.org/10.1111/gcb.15065

Sunday, J. M., Bates, A. E., & Dulvy, N. K. (2012). Thermal tolerance and the global redistribution of animals. *Nature Climate Change*, *2*(9), 686–690. https://doi.org/10.1038/nclimate1539

Suzuki, M. M., & Bird, A. (2008). DNA methylation landscapes: Provocative insights from epigenomics. In *Nature Reviews Genetics* (Vol. 9, Issue 6, pp. 465–476). https://doi.org/10.1038/nrg2341

Suzuki, M. M., Kerr, A. R. W., De Sousa, D., & Bird, A. (2007). CpG methylation is targeted to transcription units in an invertebrate genome. *Genome Research*, *17*(5), 625–631. https://doi.org/10.1101/gr.6163007

Tegner, M. J., & Dayton, P. K. (1981). *MARINE ECOLOGY-PROGRESS SERIES Population Structure, Recruitment and Mortality of Two Sea Urchins (Strongylocentrotus franciscanus and S. purpuratus) in a K e l p Forest* (Vol. 5).

Tosi, L., Aniello, F., Geraci, G., & Branno, M. (1995). DNA methyltransferase activity in the early stages of a sea urchin embryo Evidence of differential control. In *FEBS 15232 FEBS Letters* (Vol. 361).

Uthicke, S., Schaffelke, B., & Byrne, M. (2009). A boom-bust phylum? Ecological and evolutionary consequences of density variations in echinoderms. *Ecological Monographs*, *79*(1), 3–24. https://doi.org/10.1890/07-2136.1

Vaquer-Sunyer, R., & Duarte, C. M. (2011). Temperature effects on oxygen thresholds for hypoxia in marine benthic organisms. *Global Change Biology*, *17*(5), 1788–1797. https://doi.org/10.1111/j.1365-2486.2010.02343.x

Venkataraman, Y. R., Downey-Wall, A. M., Ries, J., Westfield, I., White, S. J., Roberts, S. B., & Lotterhos, K. E. (2020). General DNA Methylation Patterns and Environmentally-Induced Differential Methylation in the Eastern Oyster (Crassostrea virginica). *Frontiers in Marine Science*, *7*. https://doi.org/10.3389/fmars.2020.00225

Vezzulli, L., Colwell, R. R., & Pruzzo, C. (2013). Ocean Warming and Spread of Pathogenic Vibrios in the Aquatic Environment. In *Microbial Ecology* (Vol. 65, Issue 4, pp. 817–825). https://doi.org/10.1007/s00248-012-0163-2

Vogt, G. (2022). Studying phenotypic variation and DNA methylation across development, ecology and evolution in the clonal marbled crayfish: a paradigm for investigating epigenotype-phenotype relationships in macro-invertebrates. In *Science of Nature* (Vol. 109, Issue 1). Springer Science and Business Media Deutschland GmbH. https://doi.org/10.1007/s00114-021-01782-6

West-Eberhard, M. J. (1989). Phenotypic Plasticity and the Origins of Diversity. In *Annual Review of Ecology and Systematics* (Vol. 20). https://www.jstor.org/stable/2097092?seq=1&cid=pdf-

Whitman, D. W., & Agrawal, A. A. (2009). *What is Phenotypic Plasticity and Why is it Important?*

Williams, L., Bei, Y., Church, H. E., Dai, N., Dimalanta, E. T., Ettwiller, L. M., Evans, T. C., Langhorst, B. W., Borgaro, J. G., Guan, S., Marks, K., Menin, J. F., Nichols, N. M., Chaithanya Ponnaluri, V. K., Saleh, L., Samaranayake, M., Sexton, B. S., Sun, Z., Tamanaha, E., … Davis, T. B. (2019). *Enzymatic Methyl-seq: The Next Generation of Methylome Analysis BISULFITE SEQUENCING ALTERNATIVE METHODS FOR DETECTING 5mC AND 5hmC*.

Wilson, L. J., Fulton, C. J., Hogg, A. M., Joyce, K. E., Radford, B. T. M., & Fraser, C. I. (2016). Climate-driven changes to ocean circulation and their inferred impacts on marine dispersal patterns. In *Global Ecology and Biogeography* (Vol. 25, Issue 8, pp. 923–939). Blackwell Publishing Ltd. https://doi.org/10.1111/geb.12456

Wright, R. M., Aglyamova, G. V., Meyer, E., & Matz, M. V. (2015). Gene expression associated with white syndromes in a reef building coral, Acropora hyacinthus. *BMC Genomics*, *16*(1). https://doi.org/10.1186/s12864-015-1540-2

Xu, X., Li, G., Li, C., Zhang, J., Wang, Q., Simmons, D. K., Chen, X., Wijesena, N., Zhu, W., Wang, Z., Wang, Z., Ju, B., Ci, W., Lu, X., Yu, D., Wang, Q. F., Aluru, N., Oliveri, P., Zhang, Y. E., … Liu, J. (2019). Evolutionary transition between invertebrates and vertebrates via methylation reprogramming in embryogenesis. *National Science Review*, *6*(5), 993–1003. https://doi.org/10.1093/nsr/nwz064

Ying, H., Hayward, D. C., Klimovich, A., Bosch, T. C. G., Baldassarre, L., Neeman, T., Forêt, S., Huttley, G., Reitzel, A. M., Fraune, S., Ball, E. E., & Miller, D. J. (2022). The Role of DNA Methylation in Genome Defense in Cnidaria and Other Invertebrates. *Molecular Biology and Evolution*, *39*(2). https://doi.org/10.1093/molbev/msac018

Zemach, A., McDaniel, I. E., Silva, P., & Zilberman, D. (2010). Genome-Wide Evolutionary Analysis of Eukaryotic DNA Methylation. *Science*, *328*(5980), 916–919. https://doi.org/10.1126/science.1186366

Zhadan, P. M., Vaschenko, M. A., & Permyakov, P. A. (2021). Quantitative study of the behavior of two broadcast spawners, the sea urchins Strongylocentrotus intermedius and Mesocentrotus nudus, during mass spawning events in situ. *PeerJ*, *9*. https://doi.org/10.7717/peerj.11058